The G9a/CHCHD2/Sirt1 regulatory module acts on RNase H1 to control R-loop formation at rDNA sites

Le Li
College of Life Sciences Wuhan University
Yequn Wu
College of Life Sciences Wuhan University
Kui Dai
College of Life Sciences Wuhan University
Qing Wang
Wuhan University
Shiqi Ye
College of Life Sciences Wuhan University
Qipeng Shi
College of Life Sciences Wuhan University
Zhenfei Chen
College of Life Sciences Wuhan University
Yi-Chun Huang
College of Life Sciences Wuhan University
Weiwei Zhao
Wuhan University
Lijia Li (ljli@whu.edu.cn)
College of Life Sciences Wuhan University

Article

Keywords:

Posted Date: July 19th, 2022

DOI: https://doi.org/10.21203/rs.3.rs-1822741/v1

The G9a/CHCHD2/Sirt1 regulatory module acts on RNase H1 to control R-loop formation at rDNA sites

Le Li #, Yequn Wu #, Kui Dai, Qing Wang, Shiqi Ye, Qipeng Shi, Zhenfei Chen, Yi-Chun Huang, Weiwei Zhao, Lijia Li*

College of Life Sciences, Wuhan University, Wuhan 430072, China

# These authors contributed equally to this work

*To whom correspondence should be addressed. E-mail: ljli@whu.edu.cn Telephone: 86-27-68754505 Fax: 86-27-68754505

Abstract

R-loops are both regulators in many cellular processes and threats to genome integrity. Understanding the mechanism underlying regulation of R-loops is very important. Inspired by the findings of RNase H1-mediated R-loop formation, we focus our interest on the regulation of RNase H1 recruitment and expression. Here we report that G9a not only boosts the recruitment of RNase H1 to reduce R-loop accumulation at the rDNA site, but also positively regulates RNase H1 expression, whereas CHCHD2 prevents RNase H1 from being recruited to rDNA site and acts as a repressive transcription factor to inhibit the expression of RNase H1 to increase R-loop formation. We also found that G9a methylated the promoter of the RNase H1 gene, which inhibited the binding of CHCHD2. By contrast, when G9a was knocked down, the recruitment of CHCHD2 and Sirt1 to the RNase H1 promoter increased, which co-inhibited the RNase H1 transcription. Furthermore, G9a could directly bind CHCHD2, possibly decreasing free CHCHD2. Sirt1 could interact with CHCHD2 and functioned as a repressor suppressing transcription of the RNase H1 gene. Knockdown of Sirt1 led to binding of more G9a to the RNase H1 promoter. Taken together, we demonstrate that G9a regulates the expression of RNase H1 to maintain the steady-state balance of R-loops by suppressing CHCHD2 and Sirt1 corepressors being recruited to the target gene promoter.

Introduction

The major function of the nucleolus is to transcribe ribosomal RNA (rRNA) and to assemble ribosome subunits; this process must be tightly regulated to achieve proper cellular proliferation and growth (Boisvert et al., 2007). The rRNA transcription abundance controls ribosome biogenesis and

thus influences protein synthesis capacity, which regulates the cell growth and division rate in response to cellular stimuli (Mayer and Grummt, 2006). The rDNA gene is a region with highly active transcription, and the R-loop formation is a natural and frequent event during rRNA transcription (Aguilera and García-Muse, 2012; Grierson et al., 2012; Xu et al., 2017). R-loops consist of a nascent RNA transcript and non-coding DNA strand hybrid and a single-stranded coding DNA (Marjorie et al., 1976). R-loops as the powerful regulators play an important role in many cellular processes including gene expression regulation, transcription termination, DNA repair, telomere maintenance, Okazaki fragment maturation and immunoglobulin class-switch recombination (Skourti-Stathaki and Proudfoot, 2014). Formation of R-loops also as threats impairs DNA replication, triggers DNA damage and often causes genomic instability (Crossley et al., 2019). R-loops formed during episodes of cellular dysregulation have been linked to several human pathologies such as neurodegenerative diseases and cancer (García-Muse and Aguilera, 2019). R-loop structures could be removed from the genome by Ribonuclease H (Wahba et al., 2011), topoisomerases (Tuduri et al., 2009) and RNA helicases (Mischo et al., 2011). Specially, RNase H1 activity has been linked to the removal of R-loops in human rDNA and loss of RNase H1 causes RNA polymerase I (RNAP I) transcription-associated R-loop accumulation in the nucleus (Shen et al., 2017) . Together, these lines of evidence demonstrate that RNase H1 plays an important role in R-loop decomposition at the rDNA locus.

Dimethylated histone H3 lysine 9 (H3K9me2) is a critical epigenetic mark for gene repression and silencing (Tachibana et al., 2008) , and plays an essential role in carcinogenesis, ageing and neurodegeneration (Chen et al., 2006; Ding et al., 2013; Yuan et al., 2020; Zheng et al., 2019). Mutation of H3K9me-depositing histone methylation transferase in *Caenorhabditis elegans* shows a possible link with increased R-loops in genomic repeated elements (Zeller et al., 2016). Fragmented nucleoli are found in *Su(var)* mutant cells and the H3K9 methylation and RNAi pathways are required for the normal organization of nucleoli in *Drosophila* (Peng and Karpen, 2007). Our previous study showed that loss of H3K9me2 caused the increase in R-loop formation at the rDNA region along with the block of rRNA transcription, which in turn led to nucleoli dispersion (Zhou et al., 2020). G9a (KMT1C, EHMT2) and GLP (KMT1D, EHMT1) are two highly homologous mammalian lysine methyltransferases (KMTs), which form functional heterodimeric complexes that establish monomethylation and dimethylation on histone H3 lysine 9 (H3K9me1,

H3K9me2) in euchromatin, bearing a catalytic SET domain and ankyrin repeats involved in protein–protein interactions and methyl-lysine binding (Battisti et al., 2016; Tachibana et al., 2002; Tachibana et al., 2005). G9a facilitates transcription complex assembly and rRNA transcription due to the interaction with RNAP I and promoting changes of epigenetic marks in rDNA promoter (Yuan et al., 2007). R-loops induce antisense transcription over pause-site termination regions in mammalian protein-coding genes, which in turn leads to the generation of double-stranded RNA and the recruitment of DICER, AGO1/2 and G9a. H3K9me2 repressive mark is formed and heterochromatin protein 1γ (HP1γ) is recruited, which reinforces RNA polymerase II (RNAP II) pausing before efficient transcriptional termination (Skourti-Stathaki et al., 2014). However, the mechanism underlying G9a regulating RNAP I transcription-associated R-loop formation in human rDNA gene still needs to be further refined.

Sirt1 is a nicotinamide adenine dinucleotide (NAD+)-dependent deacetylase that is located mainly in the nucleus and involved in the regulation of the epigenetic modification, senescence, cancer and metabolism (Fang et al., 2019; Herskovits and Guarente, 2014; Rahman and Islam, 2011). Sirt1 is critically required for chromosome remodeling by deacetylating lysine residues on histones and acting on some transcription factors and cofactors (Vaquero et al., 2004). In yeast, heterochromatin formation at the ribosomal DNA (rDNA) locus is also controlled by an NAD+-dependent deacetylase Sir2p (Buck et al., 2002). A study shows that human Sirt1 suppresses the pre-rRNA levels in the nucleolus and nucleoplasmic/nucleolar shuttling is required in order for Sirt1 to act in the nucleolus (Murayama et al., 2008). Mitotic repression of RNAP I transcription correlates with transient nucleolar enrichment of Sirt1, which deacetylates TAF_I68 (another subunit of RNAP I specific transcription factor SL1). Hypoacetylation of TAF_I68 destabilizes SL1 binding to the rDNA promoter, thereby impairing transcription complex assembly (Voit et al., 2015). Taken together, epigenetic control of rDNA loci is closely related to Sirt1, but whether Sirt1 is involved in R-loop regulation during rRNA transcription remains poorly understood.

The coiled-coil-helix-coiled-coil-helix domain-containing protein 2 (CHCHD2) which is also named mitochondria nuclear retrograde regulator 1(MNRR1) is a multifunctional protein found in both the mitochondrion and the nucleus. CHCHD2 plays an important role in regulating mitochondrial metabolism and affecting synthesis of respiratory chain component (Grossman et al., 2017; Meng et al., 2017; Purandare et al., 2018). In the mitochondrion, CHCHD2 functions in a

novel way by binding to cytochrome c oxidase (COX), which stimulates respiration (Aras et al., 2015). In the nucleus, CHCHD2 as a transcription factor trans-activates nuclear coding genes and binds to a novel promoter element that contains a highly conserved motif termed the oxygen-responsive element (ORE) in the COX subunit 4 isoform 2 (COX4I2), increasing transcription at 4% oxygen (Aras et al., 2013). Based on the blast analysis of the RNase H1, G9a and Sirt1 Interaction Protein Database, we focused on CHCHD2 as intersection and speculated that it might be involved in regulating R-loop formation in human rDNA.

Here, we report that CHCHD2 suppresses recruitment and expression of RNase H1, leading to R-loop accumulation at the rDNA locus. CHCHD2 can form a complex with Sirt1, which binds to the RNase H1 promoter under depleting of G9a. By contrast, G9a is required for RNase H1 transcription because it can prevent CHCHD2 and Sirt1 from binding to the promoter, and G9a can interact with CHCHD2 to reduce free CHCHD2. Furthermore, G9a boosts the recruitment of RNase H1 to reduce R-loop accumulation at the rDNA site. Taken together, our results reveal that G9a, CHCHD2 and Sirt1 as a regulatory module act on RNase H1 to control R-loop formation at human rDNA sites.

Materials and Methods

Drug treatment

BIX 01294 (S8006), BRD4270 (S7591) and EX 527 (S15421) from Selleck (Shanghai, China) were dissolved in DMSO, respectively. Stock solutions were stored at -20°C and diluted to the respective experimental concentrations with phosphate buffer saline (PBS) prior to use.

Antibodies

Antibodies specific for fibrillarin (ab166630, Abcam, Cambridge, UK), RNaseH1 (15606-1-AP, Proteintech, Wuhan, China), CHCHD2 (CoIP: 19424-1-AP, Proteintech, Wuhan, China), CHCHD2 (IF & WB: 66302-1-Ig, Proteintech, Wuhan, China) , G9a (IF & CoIP: ab183889, Abcam, Cambridge, UK), G9a (WB: 66689-1-Ig, Proteintech, Wuhan, China), Sirt1 (07-131, Millipore, USA), α-tubulin (AF0001, Beyotime, Shanghai, China), H3 (AF0009, Beyotime, shanghai, China), H3 (ab1791, Abcam, Cambridge, UK), H3K9ac (ab10812, Abcam, Cambridge, UK), H3K9me2 (ab1220, Abcam, Cambridge, UK), DNA-RNA Hybrid S9.6 (ENH001, Kerafast, Boston, MA, USA), GST (66001-2-Ig, Proteintech, Wuhan, China), His (66005-1-Ig, Proteintech, Wuhan,

China), pan-Acetylation (3067, DIA-AN, Wuhan, China) were used in this study. The other antibodies were as follows: Cy3 Goat Anti-Mouse IgG (H+L) (A22210, Abbkine, Wuhan, China), FITC Goat Anti-Rabbit IgG (H+L) (A22120, Abbkine, Wuhan, China), Cy3 Goat Anti-Rabbit IgG (H+L) (AP132C, Sigma), FITC Goat Anti-Mouse IgG (H+L) (F0257, Sigma).

Cell culture

The HeLa cells and 293T cells were purchased from the China Center for Type Culture Collection and cultured in Dulbecco's modified Eagle's medium (DMEM) containing 10% fetal bovine serum, penicillin (20 units/mL) and streptomycin (20 units/mL). 2 μg/mL of puromycin (P012-25mg, MDBio, Qingdao, China) was added to the medium for the culture of the stable shG9a, shCHCHD2 and shSIRT1 cell lines. All cells were tested negative for cross-contamination of other human cells and mycoplasma contamination.

Plasmid and Transfection

The shRNA oligonucleotides against target genes G9a, CHCHD2-isoform1, CHCHD2-isoform2 and Sirt1 were cloned into pLKO.1-TRC Cloning vector (Addgene Plasmid 10878. Protocol Version 1.0. December 2006.). Independent shRNA oligonucleotides were designed with a 5'-*AgeI* restriction site overhang on the top strand and a 5'-*EcoRI* restriction site overhang on the bottom strand. Each strand contained hairpin loop (CTCGAG), terminator (TTTTT). Puromycin inducible shRNA was used to generate stable RNA-expressed HeLa cell lines. HeLa (2×10^5) cells were seeded into a 6-well plate and transfected with 2 μg pLKO.1-shRNA using Lipofectamine 2000 (#11668-019, Invitrogen, Carlsbad, California, USA), after which the stably transfected cells were selected in media containing 3 μg/mL of puromycin (P012-25mg, MDBio, Qingdao, China). The siRNA against Human RNase H1, Human G9a and the negative control sequence were synthesized by GenePharma (Suzhou, China). The shRNA oligonucleotide sequences and siRNA sequences were shown in **Supplementary Table 1**. The pEGFP-hG9a (Addgene ID 330025) and pEGFP-ΔSET-hG9a (Addgene ID 330026) plasmids were obtained from Addgene. The sequences for the CHCHD2-isoform1 protein were synthesized by Genewiz (Suzhou, China) and were cloned into pcDNA3.1-3flag vectors. The full-length coding sequences of target genes, CHCHD2-isoform2, Sirt1, RNase H1,were amplified from human cDNA and constructed into pcDNA3.1-3flag vectors. For the luciferase assay, human genomic DNA was prepared, and the RNase H1 promoter or CHCHD2 promoter region was inserted into the pGL3-basic vector (Promega). The promoter

sequences were amplified using the PCR primers shown in **Supplementary Table 2**. The above siRNA and plasmid transfections were carried out using Gene Twin (#TG101-02, Biomed, Beijing, China) and Lipofectamine 2000 (#11668-019, Invitrogen, Carlsbad, California, USA) respectively, according to the manufacturer's instructions. Plasmids for protein interactions: the full-length coding sequences of target genes G9a, CHCHD2-isoform1, CHCHD2-isoform2 and Sirt1 were constructed into pGADT7 or pGBKT7 vectors, respectively, for yeast two-hybrid experiments. G9a and Sirt1 were cloned into pGEX-4T-1(with GST tag), respectively, and CHCHD2-isoform1 and CHCHD2-isoform2 were cloned into pMAL-C2X vectors (with His tag), respectively, for the subsequent prokaryotic expression, purification in vitro and GST-pulldown experiments.

DRIP assay

DRIP assays were performed with some modifications according to the method reported (Ginno et al., 2012; Parajuli et al., 2017). Total nucleic acids were extracted from HeLa cells by SDS/Proteinase K treatment at 37 °C followed by phenol-chloroform extraction and ethanol precipitation. For RNase H treated controls, nucleic acids were treated with 75 U/mL of RNase H (EN0202, Thermo Scientific, Lithuania) overnight at 37ºC and re-precipitated prior to sonication. Purified DNA was resuspended in 500 ul TE buffer, and sonicated with Covaris™ S220 (with settings at Peak Power:100.0, Duty Factor: 5.0, Cycles/Burst: 200, and Avg.Power:5.0) for 2 min to generate ~250-bp-long DNA. Five micrograms of DNA were immunoprecipitated overnight at 4°C with 5 μg of S9.6 antibody in incubation buffer (20 mM Tris-HCl pH 7.5, 50 mM NaCl, 5 mM EDTA, 0.2 mM PMSF, 0.2 mM DTT). Immunoprecipitated proteins were bound to rProtein A Sepharose Fast Flow (17-1279-03, GE Healthcare, Uppsala, Sweden) for 3 h, washed three times in washing buffer (50 mM Tris-HCl pH 7.5, 10 mM EDTA, 50 mM NaCl; 100 mM NaCl; 150 mM NaCl), and then eluted with 50 mM Tris-HCl (pH 7.5), 10 mM EDTA, 50 mM NaCl, 1%SDS and 20 μg proteinase K for 60 min at 55°C. Immunoprecipitated DNA was analyzed by quantitative PCR using the primers listed in **Supplementary Table 3**. DNA in the immunoprecipitates was compared with input DNA, and the difference between untreated and RNase H-treated samples is presented as DRIP signals.

ChIP assay

ChIP was performed according to the method reported by Cong et al. (Cong et al., 2012). HeLa (8×10^5) cells were washed twice with 1×PBS after 48 h of transfection, formaldehyde fixed and then

lysed with 1 mL lysis buffer (1 mM Tris-HCl pH 7.5, 1% SDS, 0.2 mM EDTA, 0.1 mM PMSF, 0.1 mM DTT, 0.1% Protease Inhibitor Cocktail (P8340-1ML, Sigma)). The genomic DNA dissolved in lysis buffer was sonicated to 500-750 bp by ultrasonic fragmentation, of which 40 μl was used as a positive control, the remaining was divided into two and added into equal volumes of incubation buffer (consistent with the composition of the incubation buffer used in the DRIP assay), which were blocked with rProtein A Sepharose Fast Flow and Normal Rabbit Serum (BMS0090, Abbkine, Wuhan, China) to remove non-specific antibodies. After centrifugation, the supernatant was incubated overnight at 4°C with antibody and then bound with protein A for 3 h. IgG-Rb (A7016, Beyotime, Shanghai, China) was used as a negative control for mock immunoprecipitation. The precipitate after centrifugation was washed three times with a gradient of 1 mL washing buffer (consistent with the composition of the incubation buffer used in the DRIP assay), and then eluted with 60℃ preheated elution buffer (20 mM Tris-HCl pH 7.5, 50 mM NaCl, 5 mM EDTA, 0.2 mM PMSF, 0.2 mM DTT, 1% SDS). The resulting eluate was incubated with 200 mM NaCl and 20 μg of proteinase K at 55°C for 6 h for decrosslinking followed by 20 μg of RNase A for 30 min at 37 °C. The DNA was then precipitated according to the DNA purification procedure, and the precipitate was subjected to quantitative PCR using the primers shown in **Supplementary Table 3**.

Real-time quantitative PCR

RNA extraction and real-time quantitative PCR (RT-qPCR) were carried out according to the method reported (Zhou et al., 2020). Briefly, cells cultured in six-well plates were digested and lysed by 1 mL of Trizol per well, followed by extract. The RNA sample was dissolved in RNA-enzyme-free double-distilled water and frozen at -80°C for subsequent experiments. The total RNA obtained was reverse transcribed to cDNA by HiScript® II 1st Strand cDNA Synthesis Kit (R212-01/02, Vazymes, Nanjing, China), which was used as a template for real-time fluorescence quantification using iTaq Universal SYBR® Green Supermix (#1725124, Bio-Rad, California, USA) in a StepOne Plus real-time PCR system (Applied Biosystems, Carlsbad, California, USA). The amplification conditions were 95°C for 2 min, 95°C for 5 s, 59°C for 15 s and 72°C for 20 s, and the last three steps were performed for 40 cycles. The genes for double quantification controls were *GAPDH* and *β-actin*, and the primers were shown in the **Supplementary Table 4.**

Immunofluorescence staining

Immunofluorescence staining was performed as previously described (Zhou et al., 2020). Cells

cultured on slides were washed with 1×PBS to remove the medium, fixed with 4% paraformaldehyde for 10 min, washed three times with 1xPBS, permeabilized with 0.5% Triton X-100 for 25 min, washed three times with 1xPBS, blocked with 3% BSA at room temperature for 1 h, incubated with the antibody overnight at 4°C, washed three times with PBS and then combined with the secondary antibody labeled with Cy3 and FITC for 2 h at 37°C. The nuclei were detected by DAPI staining and the other fluorescence was observed by fluorescence microscopy equipped with Cy3, FITC filter.

Western blot analysis

Total proteins extracted from the treated cells using extraction buffer (100 mM Tris-HCl pH 7.5, 50 mM NaCl, 5 mM EDTA ,1 mM PMSF and 1 mM DTT) were separated by electrophoresis in a SDS-page gel. Then the proteins were transferred to PVDF membranes, blocked by 5% milk at room temperature for 2 h and incubated overnight at 4°C together with antibodies. The immunoreactive bands were observed by chemiluminescence after binding of the corresponding secondary antibody. The secondary antibodies were the horseradish peroxidase (HRP) labeled goat anti-mouse IgG (A0126, Beyotime, Shanghai, China,) and the HRP labeled goat anti-rabbit IgG (A3327, Beyotime, Shanghai, China). Immunoreactivity was determined using the ECL method (K-12045-D50, advansta, California, USA) according to the manufacturer's instructions (Zhou et al., 2021).

Luciferase reporter assays

The promoter of the target gene was constructed into the pGL3 plasmid with the firefly luciferase gene, and the plasmid phRL-TK with the renilla luciferase gene was used as a control to co-transfect into cells with the reporter gene. The total protein was obtained by lysing the cells with the lysis solution in the dual fluorescence assay kit (E1910, Promega, Madison, USA). The firefly fluorescence signal was first generated when the Luciferase Assay Reagent II was added through automatic sample injection system, after quantifying the intensity of firefly fluorescence. The Stop&Glo Reagent was added to the same sample to quench the above reaction and simultaneously initiate the renilla luciferase reaction for a second measurement, and the ratio obtained from the two measurements in the Spectramax ID5 multi-mode microplate reader (Molecular Devices, California, USA) was used for later analysis. The activity of the co-transfected TK-Renilla luciferase plasmid was used as a transfection efficiency indicator to normalize the firefly luciferase. Extracts from at least three independent transfection experiments were assayed in triplicate. The results are shown

as means ±SD (Farr and Roman, 1992; Sherf et al., 1996).

GST-Pull down

The proteins CHCHD2-1 with a His tag, CHCHD2-2 with a His tag, G9a with a GST tag and Sirt1 with a GST tag were expressed in *Escherichia coli* (BL21) and purified using the His tag protein purification kit (P2226, Beyotime, Shanghai, China) or the GST tag protein purification kit (P2262, Beyotime, Shanghai, China). The GST-Pull down assays were carried out according to the method reported by Einarson et al. (Einarson et al., 2007). The proteins carrying those two tags were incubated together with equal amounts of pulldown binding buffer (50 mM Tris-HCl pH 8.0, 250 mM NaCl, 1 mM EDTA, 1% NP-40, 10 mM $MgCl_2$, 0.2 mM PMSF and 0.2 mM DTT) and 50 μL of BeyoGold ™ GST-tag Purification resin (rinsing three times in pulldown binding buffer) for 2 h at 4°C with end-over-end mixing. Centrifuge the samples at 13,000 rpm for 10 s at 4°C in a microcentrifuge and wash the beads 6 times with 1 mL of ice-cold washing buffer (50 mM Tris-HCl pH 8.0, 300 mM NaCl, 1 mM EDTA, 1% NP-40,10 mM $MgCl_2$, 0.2 mM PMSF and 0.2 mM DTT). Discard the washes, and then detect with antibodies specific for the tag and the target protein by western blot analysis.

Co-IP assay

Co-IP was performed according to the previously described protocol (You et al., 2019). HeLa (6×10^5) Cells transfected for 48 h were digested with trypsin and collected, followed by washing twice with 1×PBS. These cells were lysed for 2 h by 1.5 mL buffer A (20 mM Tris-HCl pH 8.0, 150 mM NaCl, 5 mM EDTA, 0.5% NP-40, 0.2 mM PMSF, 0.2 mM DTT, 0.2% Protease Inhibitor Cocktail (P8340-1ML, Sigma)), centrifuged at 12,000 g for 10 min and the supernatant was extracted, of which 300 μL was used as a positive control. The remaining supernatant was blocked with 100 μL rProtein A Sepharose Fast Flow (17-1279-03, GE Healthcare, Uppsala, Sweden) for 2 h. After centrifugation, the supernatant was extracted again and divided into two equal volumes, one with 2-3 μg of the target protein antibody and one with the homologous IgG (IgG-Rb (A7016, Beyotime, Shanghai, China), IgG-mouse (Q-6004, DIA-AN, Wuhan, China)) for negative control, and mixed overnight at 4°C in an inverted shaker. Then, 50 μL rProtein A Sepharose Fast Flow was added to bind to the antibody for 2 h. The above antigen-antibody-protein A bead complex was centrifuged at 3000 g for 10 min, and the precipitate was washed with 1 mL buffer A and buffer B (20 mM Tris-HCl pH 8.0, 250 mM NaCl, 5 mM EDTA, 0.5% NP- 40, 0.2 mM PMSF, 0.2 mM DTT, 0.2% Protease Inhibitor

Cocktail) three times, respectively. The protein bound on the agarose (beads) was eluted with glycine buffer (0.2M, pH 2.2) for subsequent SDS-PAGE analysis.

In vitro and vivo acetylation detection

The acetylation detection was carried out according to the previously described protocol (You et al., 2019). Sirt1 with GST tag expressed in BL21 were in vitro incubated with the purified CHCHD2-isoform1 and CHCHD2-isoform2 proteins in the deacetylase buffer (10 mM Tris-HCl pH-8.0, 150 mM NaCl, 10% glycerol) for 2 h at 37°C. Then, the reaction was stopped by stop buffer (1 M HCl, 0.16 M acetic acid). The above components mixed with equal amounts of loading buffer were separated by electrophoresis in SDS-page gel. Sirt1 deacetylation function was detected by western blot analysis with the pan-acetylation antibody (3067, DIA-AN, Wuhan, China). The experimental procedure for in vivo acetylation detection is the same as Co-IP. After knocking down or overexpressing Sirt1 protein in HeLa cells, those cells were lysed in buffer A, then the cell lysate was mixed with acetylated lysine antibodies at 4 °C for overnight followed by the addition of rProtein A Sepharose Fast Flow. Immunocomplexes were washed by 1 mL buffer A and 1mL buffer B three times, respectively, and subjected to western blot.

Yeast two-hybrid analysis

Yeast two-hybrid analysis was performed according to the Matchmaker GAL4 Two-Hybrid System 3 manufacturer's manual (Clontech, California, USA). The target genes were constructed into the prey plasmid pGAD-T7 and the bait plasmid pGBK-T7, and the constructed vectors were co-transformed into *Saccharomyces cerevisiae* strain AH109 by using the super yeast transformation kit (SK2401-200, Coolaber, Beijing, China). Transformants were grown on synthetic medium plates (SD medium) lacking Trp and Leu (SD / -Trp-Leu) at 30°C for 2 d, and colonies with good growth status were selected, diluted with sterile water and recultured on medium plates (SD / -Trp-Leu-His -Ade).

Statistical analysis

The data and error bars were calculated from three independent experiments. The data in this manuscript were analyzed for significant differences between the experimental groups and control groups using the *t*-test which was performed using the Microsoft Excel (2019). "Two tails" was used for the calculations of *P* values. "Type 2" was chosen for equivariance hypothesis between two groups. All the results were considered statistically significant when $P < 0.05$.

Results

G9a and CHCHD2 are involved in R-loop formation by mediating the recruitment of RNase H1 at the rDNA locus

The study of R-loops and their degradation has sparked more attention in recent year, in which it has been shown that nuclear RNA–DNA hybrid levels increase upon human ribonuclease H1 depletion (Parajuli et al., 2017; Shen et al., 2017). To measure the amount of RNA–DNA hybrids in the control group versus the RNase H1-depleted or RNase H1-overexpressed group, we performed DNA–RNA immunoprecipitation (DRIP) using the well-characterized RNA–DNA hybrid antibody S9.6. We conducted a real-time quantitative PCR at the rDNA locus (**Figure 1A**), of which the 18S rRNA-coding region (amplicon H4, H4-) and 28S rRNA-coding region (amplicon H8) are the hot spot for R-loop formation, and we found that RNase H1 regulates the formation of R-loops at the well-characterized hybrid-forming site. Analysis of the DRIP-qPCR signal from RNase H1-depleted cells revealed a significant 2~fold increase at amplicon H4/H4- and a 1.45~fold increase at amplicon H8 in R-loops compared with those in siNC cells (**Figure 1B**). As expected, RNase H1-overexpressed cells showed a significant decrease in RNA–DNA hybrids compared with those in control cells (**Figure 1 C**). The specificity of the DRIP-qPCR approach was controlled by vitro treatment with RNase H, which compromised the DRIP signal (data not shown). Further dissection of the role that RNase H1 plays revealed that RNase H1 activity has been linked to the removal of R-loops in human rDNA.

Our previous studies suggested that loss of H3K9 dimethylation (H3K9me2) triggered the R-loop accumulation at the rDNA locus, which further led to the multilobed nucleoli, implying that H3K9 methyltransferase G9a was involved in regulation of the R-loop mediated structural integrity of nucleoli (Zhou et al., 2020). To investigate the G9a-mediated regulation of R-loop formation, we performed DRIP analysis at the rDNA region. Compared with the parental cells, the shG9a HeLa cells that stably suppressed G9a expression showed a significant increase in R-loop levels at the rDNA locus. Meanwhile, the cells that ectopically expressed G9a wild-type (G9a WT) showed the reduced R-loop levels at the rDNA locus; on the contrary, SET domain-deleted G9a (G9a ΔSET) failed to repress R-loop accumulation especially in amplicon H4/H8 (**Figure 1D**). Pretreatment with an in vitro RNase H enzyme led to a significant reduction of RNA–DNA hybrids in HeLa cells,

confirming the specificity of the S9.6 antibody.

In order to understand the mechanism underlying G9a-mediated regulation of R-loop formation, by blast analysis of the G9a Interaction Protein Database (Rolland et al., 2014), we found that an oxidative stress-related protein CHCHD2 (MNRR1) might be associated with G9a and involved in regulating R-loop formation. Thus, we examined the R-loop levels at the rDNA locus in the stable shCHCHD2 HeLa cells, and the DRIP-qPCR results confirmed that knockdown of CHCHD2 repressed R-loop accumulation. By contrast, over-expression of CHCHD2-isoform2 increased R-loop accumulation more than 2~fold compared with the control. Over-expression of CHCHD2-isoform1 is less effective than CHCHD2-isoform2 in promoting R-loop formation at the rDNA site, especially at the amplicon H4- (**Figure 1E**). We further observed decreased R-loop levels at the amplicon H4-/H8 of rDNA locus when CHCHD2 was knocked down in the stable shG9a HeLa cells (**Figure 1D**). As a control for specificity, we pretreated the extracted nucleic acids with RNase H enzyme in vitro to degrade existing RNA–DNA hybrids. Altogether, these results suggest that low expression of G9a or high expression of CHCHD2 lead to R-loop enrichment at the rDNA locus, and CHCHD2 functions at the downstream of G9a.

Considering that RNase H1, G9a and CHCHD2 are involved in the formation of RNA–DNA hybrids at the rDNA site, we focused our research on the relationship between RNase H1, G9a and CHCHD2. Endogenous RNase H1 ChIP showed that the recruitment of RNase H1 at the rDNA amplicon H4- was dependent on G9a regulation (**Figure 1F**). Compared with the shcon cells, the shG9a cells showed a significant decrease in RNase H1 recruitment. Meanwhile, the cells that ectopically expressed G9a WT showed a marked increase of RNase H1 occupancy; on the contrary, G9a ΔSET failed to promote RNase H1 recruitment. Interestingly, CHCHD2 also participated in the recruitment of RNase H1 at the rDNA amplicon H4- (**Figure 1G**). Knockdown of CHCHD2 boosted the recruitment of RNase H1 compared with the control, but over-expression of CHCHD2-isoform2 reduced RNase H1 occupancy more than 2~fold at the amplicon H4-. Over-expression of CHCHD2-isoform1 had no effect on attenuating recruitment of RNase H1. Together with the DRIP results, S9.6 ChIP was used to detect the R-loop levels and further supported the idea that G9a and CHCHD2 are involved in R-loop formation by mediating the recruitment of RNase H1 at the rDNA locus. Additionally, immunoprecipitation with IgG failed to precipitate RNA–DNA hybrids and RNase H1, indicating that the signals we measured were bona fide RNA–DNA hybrids and RNase H1

occupancy.

RNase H1, G9a and CHCHD2 regulate rRNA transcription and fragmented nucleoli

RNase H enzymes are endonucleases that cleave the RNA of RNA/DNA hybrids in a sequence-independent manner (Cerritelli and Crouch, 2009), thus maintaining genome stability by resolving R-loops that form during transcription (Aguilera and García-Muse, 2012). The intrinsic link between R-loop enrichment and transcription elongation arrest is more complex than it appears (Chen et al., 2017; Hraiky et al., 2000; Huertas and Aguilera, 2003). Therefore, we used RT-qPCR assay to detect the direct effect of RNase H1 on rRNA transcription (**Figure 2A**). Our results indeed showed that knockdown of RNase H1 led to inhibition of rRNA transcription and overexpression of RNase H1 up-regulated rRNA transcription (**Figure 2B, Supplementary Figure 2A**). Clearly, there is a causal relationship between RNase H1-deletion mediated R-loop enrichment and rRNA transcription elongation arrest. In addition, our previous studies suggested that the decreased expression of RNase H1 triggered the formation of multiple nucleoli (Zhou et al., 2020) and RNase H1 is implicated in bigger rDNA constriction formation (Zhou et al., 2021). Those above results further confirmed that loss of RNase H1 causes RNAP I transcription-associated R-loop accumulation along with suppressing rRNA transcription to trigger disordered and fragmented nucleoli.

Previous studies have shown that methylation of H3K9 by G9a is required for activation of RNAP I transcription (Yuan et al., 2007). As expected, the rRNA expression analysis showed that suppressing G9a expression led to a significant decrease in rRNA transcription (**Figure 2C**). However, knockdown of CHCHD2 upregulated rRNA transcription (**Figure 2E)**. When CHCHD2 was further knocked down in the stable knockdown G9a cell line, the expression of rRNA was significantly increased (**Figure 2D**). Since G9a and CHCHD2 are involved in R-loop formation by mediating the recruitment of RNase H1 at the rDNA locus. Based on the view that R-loop accumulation coupling with rRNA transcription arrest were involved in the disruption of the nucleolar structure (Zhou et al., 2020), we detected the stable shG9a HeLa cell line by using immunofluorescence staining with an antibody against the nucleolus marker fibrillarin, which is a nucleolar protein participating in pre-rRNA processing (Rodriguez-Corona et al., 2015). Generally, the normal interphase HeLa cell contains one to three nucleoli, but the nucleolar structure was

obviously fragmented and the percentage of nuclei with more than three nucleoli was substantially increased in the transient G9a knockdown HeLa cells and the stable shG9a HeLa cells (**Figure 2F**). G9a ΔSET did not reduce the proportion of cells with abnormal nucleolar morphology in the stable G9a knockdown HeLa cells compared with G9a WT (**Figure 2F**). We previously investigated the effect of the G9a enzyme-specific inhibitor BIX-01294 (BIX) on R-loop accumulation at the rDNA locus (Zhou et al., 2020). In this study, we used BIX and another G9a inhibitor BRD4770 (BRD) to inhibit the methyltransferase activity of G9a (Kubicek et al., 2007; Yuan et al., 2012). Treatment of cells using these two inhibitors resulted in obvious nucleolar dispersion (**Supplementary Figures 1A and 1B**). In addition, a high percentage of HeLa cells with multiple nucleoli can be observed after treatment with lower concentration of BIX for 3 h (**Supplementary Figure 1C**). Under the same inhibitor treatment, the transcription of rRNA was also impeded (**Supplementary Figure 2B**). These results suggest that G9a regulates rRNA transcription and structure of nucleoli in a SET-dependent manner. Simultaneously, we used the same way to detect the nucleolar structure of the transient CHCHD2 knockdown HeLa cells and the stable shCHCHD2 HeLa cells, but found there were no obvious fragmentation of nucleoli (**Figure 2G, Supplementary Figure 1D and 1E**). By contrast, high expression of CHCHD2 clearly led to nucleolus fission (**Supplementary Figure 1D and 1E**). When CHCHD2 was further knocked down in the stable shG9a cells, the percentage of nuclei with more than three nucleoli was reduced, suggesting that the original nucleolar morphology is restored by the loss of CHCHD2 (**Figure 2G**). Taken together, CHCHD2 is involved in the G9a-mediated R-loop regulation at the rDNA site, where abnormal R-loop accumulation along with persistent rRNA transcription blocks triggers disordered and fragmented nucleoli.

G9a promotes RNase H1 transcription and CHCHD2 represses its transcription

Inspired by the findings of that G9a mediates transcriptional repression as a major epigenetic silencing mechanism (Tachibana et al., 2008) and CHCHD2 plays an important role in trans-activating nuclear coding genes as a transcription factor (Aras et al., 2013), we speculated that the roles of G9a and CHCHD2 are not limited to the regulation of RNase H1 recruitment, but may even directly participate in the regulation of RNase H1 expression. As a result, we found that knockdown of G9a down-regulated RNase H1 transcription (**Supplementary Figure 2D**), and the siG9a or shG9a-#1 HeLa cells showed a decrease in H3K9me2 and RNase H1 protein levels (**Figure 3A**).

Similar results were obtained in the 293T and A549 cells (**Supplementary Figures 3C and 3D**). When we precisely controlled the expression of G9a WT in shcon HeLa cells or stable shG9a HeLa cells, a marked increase in RNase H1 protein level was observed along with the gradient up-regulation of G9a WT (**Figure 3B**). In order to explore the relationship between G9a enzyme activity and RNase H1 expression, we tested the RNase H1 mRNA level after 48 h of treatment with 10 μM BIX or 10 μM BRD, and found that the mRNA level was down-regulated (**Supplementary Figure 2C**). Interestingly, when using western blot to detect the RNase H1 protein level after 48 h of treatment with different concentrations of BIX or BRD, we found that the RNase H1 protein showed a concentration-independent decrease (**Supplementary Figure 3A**). After combined treatment of different concentrations of BIX and BRD for 24 h, the level of RNase H1 proteins showed a significant decrease, especially in the combined treatment of 5 μM BIX and 10 μM BRD (**Supplementary Figure 3B**). To confirm the importance of G9a HMTase activity in activating RNase H1, we transfected the stable G9a knockdown HeLa cells with G9a WT or G9a ΔSET expression plasmids. We found that G9a ΔSET group did not show increased RNase H1 expression whereas the G9a WT group increased its expression (**Figure 3C**), indicating that G9a-mediated up-regulation of RNase H1 expression is dependent on its HMTase activity. Taken together, these results suggest that G9a positively regulates expression of RNase H1 in a SET-dependent manner.

Our results also showed that knockdown of CHCHD2 led to an increase in RNase H1 transcription (**Supplementary Figure 2F**). In addition, knockdown of CHCHD2 in the stable shG9a cells also caused an increase in RNase H1 transcription (**Supplementary Figure 2E**). Consistent with the RT-qPCR, the western blot results showed that RNase H1 levels were increased after knockdown of CHCHD2 (**Figure 3D**) whereas RNase H1 expression was repressed by CHCHD2 overexpression (**Figure 3E**). When the expression of CHCHD2 was restored in the stable shCHCHD2 HeLa cells, the RNase H1 protein returned to normal levels (**Figure 3F**). Specially, the CHCHD2-isoform1 showed no effect on the expression of RNase H1. After overexpressing CHCHD2-isoform2 in shcon HeLa cells, stable shG9a HeLa cells and G9a WT rescued shG9a HeLa cells, the western blot results indicated that overexpression of CHCHD2-isoform2 could further reduce the RNase H1 protein levels (**Figure 3G**). These results show that knockdown of G9a or overexpression of CHCHD2 down-regulates RNase H1.

To further understand the mechanisms underlying RNase H1 transcriptional regulation via G9a

and CHCHD2, we conducted a luciferase reporter assay using RNase H1-promoter-luc reporter system. We first cloned three fragments with different RNase H1 promoter lengths and engineered these RNase H1 promoter fragments into pGL3 basic luciferase reporter vectors (**Figure 4A**). Then, we selected the pGL3-RH1-pro2-luc with the highest promoter activity for subsequent luciferase assay **(Figure 4B**). Consistent with RT-qPCR and western blot results, RNase H1 transcription was stimulated by depletion of CHCHD2 and repressed by overexpression of CHCHD2 (**Figure 4C**). The inhibitory effect of CHCHD2-isoform1 is not as obvious as that of CHCHD2-isoform2. Similarly, we used the RNase H1-luc reporter system to examine G9a-mediated transcriptional regulation of RNase H1. RNase H1 transcription was repressed by depletion of G9a and activated by the overexpression of G9a WT but not G9a ΔSET, and the treatment with BIX could attenuate the activation of RNase H1 transcription triggered by G9a WT (**Figure 4D**). After overexpressing CHCHD2-isoform2 in shcon HeLa cells, stable shG9a HeLa cells and G9a WT rescued shG9a HeLa cells, the results of the relative luciferase activity of RNase H1 were consistent with the western blot results (**Figure 3G**) and indicated that RNase H1 was positively regulated by G9a and the overexpression of CHCHD2-isoform2 could further reduce the expression level of RNase H1 (**Figure 4E**). On the contrary, knockdown of CHCHD2 further increased the RNase H1 expression level compared with the control group (**Figure 4F**). In addition, we performed RNase H1-luc reporter assay with stable shCHCHD2 HeLa cells to investigate whether the G9a had any effect on CHCHD2-mediated transcriptional repression of RNase H1. Overexpression of G9a abolished the RNase H1 transcriptional repression induced by CHCHD2, and knockdown of G9a could further strengthen CHCHD2-mediated RNase H1 transcriptional repression (**Figure 4G**). These results strongly suggested that negative regulation of RNase H1 transcription by CHCHD2 was dependent on the depletion of G9a.

CHCHD2 interacts with G9a and is deacetylated by Sirt1

Blast analysis of the G9a Interaction Protein Database suggested that G9a could interact with CHCHD2. Thus, we examined the interaction of G9a and CHCHD2 through several experiments. The co-localization of CHCHD2 and G9a in the HeLa cell nuclei was confirmed by using immunofluorescence staining with the CHCHD2 monoclonal antibody (66302-1-Ig) and the G9a polyclonal antibody (ab183889) (**Figure 5A**). When using the His antibody or the CHCHD2 antibody to detect GST-G9a pull-down products, a specific band was displayed at a position that

was consistent with the size of input MBP-CHCHD2-His, revealing that both CHCHD2-isoform1 and CHCHD2-isoform2 could interact specifically with G9a in vitro (**Figure 5B**). After G9a was immunoprecipitated from HeLa cells with the G9a polyclonal antibody, CHCHD2 was detected in the precipitate at the same position as the input, showing that CHCHD2 could interact with G9a in vivo (**Figure 5C**).We constructed yeast two-hybrid system bait and prey vectors to confirm the importance of G9a HMTase activity domain for direct interaction with CHCHD2. Interestingly, the direct interaction between CHCHD2-isoform2 and G9a showed a clear SET domain dependency (**Supplementary Figure 4A**). However, G9a ΔSET and CHCHD2-isoform1 still have a certain weak interaction compared with interaction between G9a WT and CHCHD2-isoform1. In the GST-pull-down system, we verified that CHCHD2-isoform1 and CHCHD2-isoform2 could directly interact with G9a depended on the G9a SET domain. Once the SET domain was destroyed, this interaction collapsed (**Supplementary Figure 4B**).

LC MALDI-TOF/TOF MS/MS analysis have identified that CHCHD2 is the interacting protein of Sirt1 (Law et al., 2009). The co-localization of CHCHD2 and Sirt1 in the HeLa cell was also confirmed by using immunofluorescence staining with the CHCHD2 monoclonal antibody (66302-1-Ig) and the Sirt1 polyclonal antibody (07-131) (**Figure 5D**). A yeast two-hybrid experiment (**Supplementary Figure 5**) and a GST pulldown assay (**Figure 5E**) further verified that CHCHD2 was the interacting protein of Sirt1. Then, we purified and incubated the recombinant MBP-CHCHD2-His protein and the GST-Sirt1 protein to construct a deacetylation reaction system in vitro. A specific band was displayed using the Anti-Acetylated-Lysine antibody at a position that was consistent with the size of input MBP-CHCHD2-His in the GST empty protein reaction products, suggesting that CHCHD2 in the prokaryotic expression system could be acetylated. Comparing with the GST empty protein, the addition of GST-Sirt1 could significantly reduce the lysine acetylation level of MBP-CHCHD2-His, indicating that Sirt1 directly deacetylated CHCHD2 (**Figure 5F**). To further confirm that CHCHD2 is the target of Sirt1-induced deacetylation in vivo, we used the stable shSirt1 HeLa cell to perform lysine acetylation immunoprecipitation. Knockdown of Sirt1 increased the basal acetylation level of endogenous CHCHD2, exogenous CHCHD2-isoform1 and CHCHD2-isoform2. The acetylation could also be retrieved to the normal level by re-introduction of Sirt1 into the stable shSirt1 HeLa cells (**Figure 5G**). Taken together, these results suggest that CHCHD2 interacts with G9a and is deacetylated by Sirt1.

Sirt1 functions as a co-repressor in regulating RNase H1

The DRIP analysis result showed that knockdown of Sirt1 reduced the R-loop levels whereas overexpression of Sirt1 showed a significant promotion for the R-loop accumulation especially in rDNA amplicon H4/H4-/H8, which was similar to that obtained from CHCHD2 (**Figures 6A**). Pretreatment with RNase H enzyme in vitro confirmed the specificity of the S9.6 antibody. Endogenous RNase H1 ChIP showed that knockdown of Sirt1 boosted the recruitment of RNase H1compared with the control, but over-expression of Sirt1 reduced RNase H1 occupancy almost 2~fold at the amplicon H4- (**Figures 6B**). IgG control group confirmed the reliability of the ChIP signals we measured. Some studies showed that human Sirt1 suppresses the pre-rRNA levels in the nucleolus (Murayama et al., 2008; Voit et al., 2015). As expected, the rRNA expression analysis showed that treatment with a kind of selective Sirt1 inhibitor EX 527 (Solomon et al., 2006) and transfection with shRNA oligonucleotides (shSirt1-#3) to suppress Sirt1 expression both led to a significant increase in rRNA transcription, especially when the inhibitor and shSirt1-#3 were treated together (**Figures 6C**). The results suggest that Sirt1 plays a same role as CHCHD2 in regulating R-loop formation and RNase H1 recruitment at rDNA sites, as well as rRNA transcription.

We next examined whether Sirt1 was involved in transcriptional regulation of RNase H1. The RT-qPCR and western blot results showed that loss of Sirt1 increased expression of RNase H1 (**Figures 6D and 6E**). When we precisely controlled the expression of Sirt1 in shcon HeLa cells or stable shSirt1 HeLa cells, a marked decrease in the RNase H1 protein level was observed along with the gradient up-regulation of Sirt1 (**Figure 6F, Supplementary Figure 3E**). We further used the RNase H1-luc reporter system to examine Sirt1-mediated transcriptional regulation of RNase H1. RNase H1 transcription was repressed by Sirt1 overexpression in the stable shSirt1 HeLa cell, and the treatment with EX 527 could attenuate the inhibition of RNase H1 transcription triggered by Sirt1 (**Figure 6G**). Simultaneously, we examined whether CHCHD2 was involved in Sirt1-mediated transcriptional regulation of RNase H1. When overexpressing CHCHD2-isoform2 in shcon HeLa cells, stable shSirt1 HeLa cells and Sirt1 rescued shSirt1 HeLa cells, western blot results indicated that CHCHD2-isoform2 could further reduce the protein level of RNase H1 (**Figure 6H**), suggesting that CHCHD2 could cooperate with Sirt1 to inhibit the expression of RNase H1.

We then tested the connection between G9a and Sirt1 in influence of RNase H1 expression. The results of RNase H1-luc reporter assay in stable shG9a HeLa cells showed that G9a promoted

RNase H1 transcription, but overexpression of Sirt1 further abolished the RNase H1 transcriptional activation induced by G9a, and the shSirt1 group had a significant recovery in RNase H1 transcriptional repression (**Supplementary Figure 6B**). Similarly, the results of RNase H1-luc reporter assay in stable shSirt1 HeLa cells showed that Sirt1 repressed RNase H1 transcription, but overexpression of G9a showed slight recovery of the Sirt1-mediated transcriptional inhibition of RNase H1. Knockdown of G9a further strengthen Sirt1-mediated RNase H1 transcriptional repression (**Supplementary Figure 6C**). In addition, we performed a RNase H1-luc reporter assay in stable shCHCHD2 HeLa cells to further investigate whether G9a or Sirt1 had any effect on CHCHD2-mediated transcriptional repression of RNase H1. After transfected with OESirt1 or G9a WT for 24 h, the shSirt1-#3 or shG9a-#1 were added into the transfection system for another 24 h. The results showed that CHCHD2 indeed repressed RNase H1 transcription. Overexpression of Sirt1 further strengthened CHCHD2-mediated RNase H1 transcriptional repression. Knockdown of Sirt1 partially restored the RNase H1 transcriptional repression compared with OESirt1, strongly suggesting that Sirt1 was involved in CHCHD2-induced RNase H1 transcriptional repression (**Supplementary Figure 6A**). Notably, overexpression of G9a abolished the RNase H1 transcriptional repression induced by CHCHD2, and shG9a could further strengthen the kind of transcriptional repression (**Figure 4G , Supplementary Figure 6A**).

CHCHD2 transcriptional regulation mediated by G9a and Sirt1

Interestingly, knockdown of G9a also resulted in upregulation of CHCHD2 which further supported the negative regulation of RNase H1 expression by CHCHD2 (**Figures 3A, 3B and 3C, Supplementary Figure 3C and 3D**). Thus, we conducted luciferase reporter assay using a CHCHD2-luc reporter system to examine G9a-mediated transcriptional regulation of CHCHD2. We cloned three fragments with different CHCHD2 promoter lengths and engineered these CHCHD2 promoter fragments into pGL3 basic luciferase reporter vectors (**Figure 7A**). Then, we selected the pGL3-CHCHD2-pro2-luc with the highest promoter activity for subsequent luciferase assay (**Figure 7B**). The results showed that CHCHD2 transcription was upregulated by depletion of G9a and repressed by G9a overexpression in the stable shG9a HeLa cells (**Figure 7C**). Simultaneously, G9a ΔSET did not significantly repress the expression of CHCHD2 compared with G9a WT, indicating that G9a regulated CHCHD2 in a SET-dependent manner (**Figure 7C**). Sirt1 functions as a co-repressor in CHCHD2-mediated regulation of RNase H1, but it is worth noting that

knockdown of Sirt1 also resulted in upregulation of CHCHD2 (**Figures 6D, 6E and 6F, Supplementary Figure 3E**), and we used the same CHCHD2-luc reporter system to examine Sirt1-mediated transcriptional regulation of CHCHD2 (**Figure 7A and 7B**). Consistent with the western blot results, CHCHD2 transcription was stimulated by depletion of Sirt1 and repressed by Sirt1 overexpression (**Figure 7D**).

G9a prevents CHCHD2 from being recruited to the promoter of the RNase H1

To further elucidate the mechanisms underlying RNase H1 transcriptional regulation by G9a, Sirt1 and CHCHD2, we performed the ChIP analysis with RT-qPCR using corresponding stable knockdown HeLa cells. We analyzed the RNase H1 promoter sequence to identify possible transcription factor binding sites. The histone modification of the RNase H1 promoter region was discovered in the ChIP-seq public database Cistrome Data Browser, and RT-qPCR primers for ChIP analysis were designed for the H3K9ac and H3K9me2 enrichment peak positions of the RNase H1 promoter region (**Supplementary Figure 7A**). The final primers RH pro A, B and C covered the distal, middle and proximal regions of the RNase H1 promoter (**Figure 8A**). First, we observed decreased G9a recruitment as well as decreased levels of H3K9me2 on the RNase H1 promoter in stable shG9a HeLa cells whereas G9a was highly recruited to the RNase H1 promoter and H3K9me2 levels increased when G9a was overexpressed (**Figure 8B**). Interestingly, the CHCHD2 and Sirt1 recruitment both increased (almost ~2.5 fold and ~3 fold) when G9a was knocked down. Then, we overexpressed G9a in the stable shG9a HeLa cells and observed that CHCHD2 and Sirt1 recruitment on the RNase H1 promoter was decreased significantly. The H3K9ac levels on the promoter region of RNase H1 also changed with the change of Sirt1 enrichment (**Figure 8B**). These results suggest that high expression of G9a along with high level of H3K9me2 prevent CHCHD2 and Sirt1 from accessing the RNase H1 promoter to activate RNase H1.

Furthermore, in the absence of Sirt1, the H3K9ac level on the RNase H1 promoter was significantly upregulated, and more G9a was bound to the RNase H1 promoter, which led to increased levels of H3K9me2. On the contrary, overexpression of Sirt1 resulted in significant reduction of G9a binding and H3K9me2 levels on the RNase H1 promoter (**Figure 8C**).Significantly, restoration of Sirt1 expression promoted CHCHD2 enrichment in the RNase H1 proximal promoter region (RH proC), whereas loss of Sirt1 inhibited recruitment of CHCHD2. However, no changes in CHCHD2 levels were observed in the RNase H1 middle promoter region (RH proB) after

knockdown of Sirt1 (**Figure 8C**). These findings demonstrated that Sirt1 or CHCHD2 and G9a competed to bind to the RNase H1 promoter regions. Sirt1 cooperated to promote CHCHD2 recruitment only in the proximal region of the RNase H1 promoter

Discussion

R-loops are involved in many cellular processes in physiological contexts, such as gene expression, transcription termination, DNA repair, telomere maintenance, Okazaki fragment maturation and immunoglobulin class-switch recombination (Crossley et al., 2019; Skourti-Stathaki and Proudfoot, 2014). But R-loops are also considered as a double-edged sword which is a source of replication stress and genome instability causing DNA damage like DSBs accumulation (Uruci et al., 2021). The nucleolus functions as an emerging hub in maintenance of genome stability and cancer pathogenesis (Lindström et al., 2018). There is an increased demand for ribosomes in highly proliferating cancer cells, and the rRNA transcription and ribosome production regulated by RNAP I in the nucleolus are invariably up-regulated in cancer (Drygin et al., 2010; Hein et al., 2013). Thus, the highly proliferating cancer cells show the enlarged nucleolus and an increased number of nucleoli (Derenzini et al., 2009; Derenzini et al., 2000). The rDNA gene is a highly active transcription region, and the R-loop formation is a natural and frequent event during rRNA transcription (Aguilera and García-Muse, 2012; Grierson et al., 2012; Xu et al., 2017). R-loops have shown to be associated with nucleolus fragmentation and rRNA transcription elongation (El Hage et al., 2010; Hraiky et al., 2000; Zhou et al., 2020). However, the exact molecular mechanism underlying R-loop formation at the rDNA sites remains largely unclear. In this study, our findings reveal a novel molecular and genetic mechanism that the G9a/CHCHD2/Sirt1 regulatory module acts on expression and recruitment of RNase H1 to control R-loop accumulation at rDNA sites.

RNase H, topoisomerases and RNA helicases have been found to be part of R-loop degradation machinery associated with the decrease of RNA: DNA hybrids in mammalian (Cristini et al., 2018; Parajuli et al., 2017; Song et al., 2017; Yang et al., 2014). Top1 and RNase H1 are partially functionally redundant in mammalian cells to suppress RNAP I transcription-associate R-loop formation and RNase H1 enriches in nucleoli to co-localize with R-loops in cultured human cells (Shen et al., 2017). Excessive R-loop formation can impede transcription elongation (Aguilera and Gómez-González, 2008; Huertas and Aguilera, 2003). The absence of RNase H1 in Top1 depleted

Escherichia coli or yeast increases the accumulation of RNA/DNA hybrids which impedes efficient transcription elongation during rRNA synthesis (El Hage et al., 2010; Hraiky et al., 2000). Our analysis of rRNA transcript levels in RNase H1 knockdown or overexpression HeLa cells further supports the notion that RNase H1-deletion-mediated R-loop enrichment was associated with rRNA transcription elongation arrest. However, there is a generally accepted view that R-loops are dynamic coupling with transcriptional pausing at gene promoters (Chen et al., 2017) and increased RNAP II pausing is often correlated with increased R-loop levels (Shivji et al., 2018; Zhang et al., 2017), whereas efficient transcription elongation prevents R-loop formation (Edwards et al., 2020). Treatment with RNAP I transcription inhibitor led to the increased R-loops levels at rDNA sites (Zhou et al., 2020). Due to characteristic of tandem repeats of rDNA, genome-wide R-loop detection technologies have mostly chosen to filter out rDNA data to improve resolution (Lin et al., 2022). A feasible way is using the alignment approach of Zentner and colleagues to align DRIP-seq reads to the rDNA repeating unit (Nadel et al., 2015; Zentner et al., 2011). In this study, we chose to analyze R-loop enrichment and endogenous RNase H1 recruitment at human rDNA loci by classical relative quantification of DRIP-qPCR and ChIP-qPCR, and selected multiple hot spots with DNA: RNA hybridization signatures to increase data coverage. Endogenous RNase H1 ChIP showed that the rDNA amplicon H4/H4- (5' region of 18S) exhibited higher levels of RNase H1 recruitment (**Figure 1F, 1G and 6B, Supplementary Figure 8**), which degrade the R-loop to ensure efficient transcription extension. As well as RNase H1 recruitment, the precise regulation of RNase H1 expression is also very pivotal. RNaseH1 is highly conserved in evolution and expressed ubiquitously in human cells and tissues (Wu et al., 1998). There is no significant difference in expression in various human tissues and it is generally used as a housekeeping gene (Cerritelli and Crouch, 1998). RNase H1 synthesis is subjected to translational regulation which are affected by two in-frame AUG codons (M1 and M27) of a single mRNA and a potent upstream open reading frame (uORF) (Suzuki et al., 2010). During normal cell growth and development, the expression of RNase H1 undergoes sensitive and subtle changes to meet the need of R-loops for maintaining a stable genome level, and subcellular distribution and levels of RNase H1 are fine-tuned in cells to maintain genome integrity (Shen et al., 2017). The current studies identify the G9a as a positive regulator and CHCHD2 as a negative regulator of RNase H1 expression, which is associated with R-loop formation and rRNA transcription at rDNA sites. Sirt1 is also participated in regulation of

RNase H1 transcription as a co-repressor.

H3K9 HMTase G9a catalyzes the mono- and dimethylation of the histone H3K9 and always mediates transcriptional repression as a major epigenetic silencing mechanism (Tachibana et al., 2008). Generally, G9a inhibits gene expression by forming histone hypermethylation at the promoter to prevent transcriptional factors from being recruited (Mozzetta et al., 2014; Roopra et al., 2004; Wang et al., 2013). It has been reported that G9a is recruited to the UHRF1 promoter along with YY1 to function as a corepressor of the target gene (Kim et al., 2015). Our results showed that G9a-mediated hypermethylation of the RNase H1 promoter contributed to transcription of the target gene, which could suppress repressor binding. Furthermore, we identified a factor, CHCHD2 as the repressor of RNase H1 transcription. CHCHD2 plays an important role in trans-activating nuclear coding genes as a transcription factor (Aras et al., 2013), regulating mitochondrial metabolism (Aras et al., 2015; Grossman et al., 2017; Purandare et al., 2018) and affecting synthesis of respiratory chain component (Meng et al., 2017). ChIP analysis showed that G9a could bind to and methylate the promoter of the RNase H1 gene, which inhibited CHCHD2 binding. By contrast, when G9a was knocked down, the decreased expression of G9a resulted in a reduction of H3K9me2 markers at the promoter of the RNase H1 gene, which was conducive to the recruitment of CHCHD2 to suppress RNase H1 expression. We also found that G9a could directly interact with CHCHD2 which possibly decreased free CHCHD2. Previous studies have predicted that CHCHD2 is a target of Sirt1-induced deacetylation (Aras et al., 2020). Our results revealed that Sirt1 could indeed interact with and deacetylate CHCHD2. We found that loss of G9a led to the recruitment of more Sirt1 as well as more CHCHD2 to the RNase H1 promoter to co-suppress transcription of the RNase H1 gene (**Figure 9**). By the contrary, loss of Sirt1 led to binding of more G9a to the RNase H1 promoter due to the increase of H3K9ac markers at the promoter of the RNase H1 gene. The enrichment trends of factors in the G9a/CHCHD2/Sirt1 functional module were almost the same in each RNase H1 promoter region. However, when the expression level of Sirt1 changed, the significant effect on the recruitment level of CHCHD2 was only manifested in the RNase H1 proximal promoter region. The RNase H1 distal promoter region was not considered because the changes in Sirt1 enrichment and H3K9me2 levels were not significant in the three groups of control experiments. After knockdown of Sirt1, although G9a and corresponding H3K9me2 levels increased, no changes in CHCHD2 levels were observed in the RNase H1 middle promoter region,

which could be because Sirt1 negatively regulated the expression of CHCHD2 **(Figures 6D, 6E and 6F, Figure 7D, Supplementary Figure 3E)**.

In summary, this study showed that G9a boosts the recruitment of RNase H1 and positively regulates RNase H1 expression whereas CHCHD2 suppresses RNase H1 recruitment and acts as a repressive transcription factor to inhibit the expression of RNase H1 to increase R-loop formation at the rDNA site. CHCHD2 can form a complex with Sirt1 as the co-repressor, which binds to the RNase H1 promoter under depleting of G9a. These findings provide a possible strategy to regulate R-loop formation, rRNA transcription and cancer cell growth through co-targeting G9a, CHCHD2 and Sirt1.

Declarations

Ethics approval and consent to participate Not applicable.

Consent for publication Not applicable.

Availability of data and materials All data generated or analyzed during this study are included in this published article and its supplementary information files or are available upon request.

Competing interests The authors declare that they have no competing interests.

Funding This work was supported by the National Natural Science Foundation of China (No. 31871238). The funders had no role in the study design, data collection and analysis, decision to publish, or preparation of the manuscript.

Authors' contributions Le L., Y.W., K.D., Q.W., S.Y., Q.S., Y.H. performed experiments. L.L., Le L., Y.W., K.D., W.Z. planned and analyzed experiments. Le L., Y.W., Q.W., Z.C. helped with data analysis. L.L., Le L., Y.W. wrote and edited the manuscript. L.L., Le L. conceived the study.

Acknowledgements Not applicable.

Reference

Aguilera, A., and García-Muse, T. (2012). R Loops: From transcription byproducts to threats to genome stability. Molecular Cell *46*, 115-124.

Aguilera, A., and Gómez-González, B. (2008). Genome instability: a mechanistic view of its causes and consequences. Nature Reviews Genetics *9*, 204-217.

Aras, S., Bai, M., Lee, I., Springett, R., Hüttemann, M., and Grossman, L.I. (2015). MNRR1 (formerly CHCHD2) is a bi-organellar regulator of mitochondrial metabolism. Mitochondrion *20*, 43-51.

Aras, S., Pak, O., Sommer, N., Finley Jr, R., Hüttemann, M., Weissmann, N., and Grossman, L.I. (2013). Oxygen-dependent expression of cytochrome c oxidase subunit 4-2 gene expression is mediated by transcription factors RBPJ, CXXC5 and CHCHD2. Nucleic Acids Research *41*, 2255-2266.

Aras, S., Purandare, N., Gladyck, S., Somayajulu-Nitu, M., Zhang, K., Wallace, D.C., and Grossman, L.I. (2020). Mitochondrial Nuclear Retrograde Regulator 1 (MNRR1) rescues the cellular phenotype of MELAS by inducing homeostatic mechanisms. Proceedings of the National Academy of Sciences of the United States of America *117*, 32056-32065.

Battisti, V., Pontis, J., Boyarchuk, E., Fritsch, L., Robin, P., Ait-Si-Ali, S., and Joliot, V. (2016). Unexpected Distinct Roles of the Related Histone H3 Lysine 9 Methyltransferases G9a and G9a-Like Protein in Myoblasts. Journal of Molecular Biology *428*, 2329-2343.

Boisvert, F.-M., van Koningsbruggen, S., Navascués, J., and Lamond, A.I. (2007). The multifunctional nucleolus. Nature Reviews Molecular Cell Biology *8*, 574-585.

Buck, S.W., Sandmeier, J.J., and Smith, J.S. (2002). RNA Polymerase I propagates unidirectional spreading of rDNA silent chromatin. Cell *111*, 1003-1014.

Cerritelli, S.M., and Crouch, R.J. (1998). Cloning, expression, and mapping of Ribonucleases H of human and mouse related to bacterial RNase HI. Genomics *53*, 300-307.

Cerritelli, S.M., and Crouch, R.J. (2009). Ribonuclease H: the enzymes in eukaryotes. FEBS Journal *276*, 1494-1505.

Chen, H., Yan, Y., Davidson, T.L., Costa, M., and Shinkai, Y. (2006). Hypoxic stress induces dimethylated histone H3 lysine 9 through histone methyltransferase G9a in mammalian cells. Cancer Research *66*, 9009-9016.

Chen, L., Chen, J.-Y., Zhang, X., Gu, Y., Xiao, R., Shao, C., Tang, P., Qian, H., Luo, D., Li, H.*, et al.* (2017). R-ChIP using inactive RNase H reveals dynamic coupling of R-loops with transcriptional pausing at gene promoters. Molecular Cell *68*, 745-757.

Cong, R., Das, S., Ugrinova, I., Kumar, S., Mongelard, F., Wong, J., and Bouvet, P. (2012). Interaction of nucleolin with ribosomal RNA genes and its role in RNA polymerase I transcription. Nucleic acids research *40*, 9441-9454.

Cristini, A., Groh, M., Kristiansen, M.S., and Gromak, N. (2018). RNA/DNA hybrid interactome identifies DXH9 as a molecular player in transcriptional termination and R-Loop-associated DNA damage. Cell Reports *23*, 1891-1905.

Crossley, M.P., Bocek, M., and Cimprich, K.A. (2019). R-Loops as cellular regulators and genomic threats. Molecular Cell *73*, 398-411.

Derenzini, M., Montanaro, L., and Treré, D. (2009). What the nucleolus says to a tumour pathologist. Histopathology *54*, 753-762.

Derenzini, M., Trerè, D., Pession, A., Govoni, M., Sirri, V., and Chieco, P. (2000). Nucleolar size indicates the rapidity of cell proliferation in cancer tissues. Journal of Pathology *191*, 181-186.

Ding, J., Li, T., Wang, X., Zhao, E., Choi, J.-H., Yang, L., Zha, Y., Dong, Z., Huang, S., Asara, John M.*, et al.* (2013). The Histone H3 Methyltransferase G9A epigenetically activates the Serine-Glycine synthesis pathway to sustain cancer cell survival and proliferation. Cell Metabolism *18*, 896-907.

Drygin, D., Rice, W.G., and Grummt, I. (2010). The RNA polymerase I transcription machinery: an emerging target for the treatment of cancer. Annual review of pharmacology and toxicology *50*, 131-156.

Edwards, D.S., Maganti, R., Tanksley, J.P., Luo, J., Park, J.J.H., Balkanska-Sinclair, E., Ling, J., and Floyd, S.R. (2020). BRD4 prevents R-Loop formation and transcription-replication conflicts by ensuring efficient transcription elongation. Cell Reports *32*.

Einarson, M.B., Pugacheva, E.N., and Orlinick, J.R. (2007). GST Pull-down. CSH protocols *2007*, pdb.prot4757.

El Hage, A., Tollervey, D., French, S.L., and Beyer, A.L. (2010). Loss of Topoisomerase I leads to R-loop-mediated transcriptional blocks during ribosomal RNA synthesis. Genes and Development *24*, 1546-1558.

Fang, Y., Tang, S., and Li, X. (2019). Sirtuins in metabolic and epigenetic regulation of stem cells. Trends in Endocrinology & Metabolism *30*, 177-188.

Farr, A., and Roman, A. (1992). A pitfall of using a second plasmid to determine transfection efficiency. Nucleic acids research *20*, 920.

García-Muse, T., and Aguilera, A. (2019). R Loops: From physiological to pathological roles. Cell *179*, 604-618.

Ginno, Paul A., Lott, Paul L., Christensen, Holly C., Korf, I., and Chédin, F. (2012). R-Loop formation is a distinctive characteristic of unmethylated human CpG island promoters. Molecular Cell *45*, 814-825.

Grierson, P.M., Lillard, K., Behbehani, G.K., Combs, K.A., Bhattacharyya, S., Acharya, S., and Groden, J. (2012). BLM helicase facilitates RNA polymerase I-mediated ribosomal RNA transcription. Human Molecular Genetics *21*, 1172-1183.

Grossman, L.I., Purandare, N., Arshad, R., Gladyck, S., Somayajulu, M., Hüttemann, M., and Aras, S. (2017). MNRR1, a biorganellar regulator of mitochondria. Oxidative Medicine & Cellular Longevity, 1-12.

Hein, N., Hannan, K.M., George, A.J., Sanij, E., and Hannan, R.D. (2013). The nucleolus: an emerging target for cancer therapy. Trends in Molecular Medicine *19*, 643-654.

Herskovits, A.Z., and Guarente, L. (2014). SIRT1 in neurodevelopment and brain senescence. Neuron *81*, 471-483.

Hraiky, C., Drolet, M., and Raymond, M.-A. (2000). RNase H overproduction corrects a defect at the level of transcription elongation during rRNA synthesis in the absence of DNA topoisomerase I in *Escherichia coli*. Journal of Biological Chemistry *275*, 11257-11263.

Huertas, P., and Aguilera, A. (2003). Cotranscriptionally formed DNA:RNA hybrids mediate transcription elongation impairment and transcription-associated recombination. Molecular Cell *12*, 711-721.

Kim, K.-B., Son, H.-J., Choi, S., Hahm, J.Y., Jung, H., Baek, H.J., Kook, H., Hahn, Y., Kook, H., and Seo, S.-B. (2015). H3K9 methyltransferase G9a negatively regulates UHRF1 transcription during leukemia cell differentiation. Nucleic acids research *43*, 3509-3523.

Kubicek, S., O'Sullivan, R.J., August, E.M., Hickey, E.R., Zhang, Q., Teodoro, M.L., Rea, S., Mechtler, K., Kowalski, J.A., Homon, C.A.*, et al.* (2007). Reversal of H3K9me2 by a small-molecule inhibitor for the G9a histone methyltransferase. Molecular cell *25*, 473-481.

Law, I.K.M., Liu, L., Xu, A., Lam, K.S.L., Vanhoutte, P.M., Che, C.-M., Leung, P.T.Y., and Wang, Y. (2009). Identification and characterization of proteins interacting with SIRT1 and SIRT3: implications in the anti-aging and metabolic effects of sirtuins. PROTEOMICS *9*, 2444-2456.

Lin, R., Zhong, X., Zhou, Y., Geng, H., Hu, Q., Huang, Z., Hu, J., Fu, X.-D., Chen, L., and Chen, J.-Y. (2022). R-loopBase: a knowledgebase for genome-wide R-loop formation and regulation. Nucleic Acids Research *50*, D303-D315.

Lindström, M.S., Jurada, D., Bursac, S., Orsolic, I., Bartek, J., and Volarevic, S. (2018). Nucleolus as an emerging hub in maintenance of genome stability and cancer pathogenesis. Oncogene *37*, 2351.

Marjorie, T., Raymond, L.W., and Ronald, W.D. (1976). Hybridization of RNA to Double-Stranded DNA:

Formation of R-Loops. Proceedings of the National Academy of Sciences of the United States of America *73*, 2294.

Mayer, C., and Grummt, I. (2006). Ribosome biogenesis and cell growth: mTOR coordinates transcription by all three classes of nuclear RNA polymerases. Oncogene *25*, 6384-6391.

Meng, H., Yamashita, C., Shiba-Fukushima, K., Inoshita, T., Funayama, M., Sato, S., Hatta, T., Natsume, T., Umitsu, M., Takagi, J.*, et al.* (2017). Loss of Parkinson's disease-associated protein CHCHD2 affects mitochondrial crista structure and destabilizes cytochrome c. Nature communications *8*, 15500.

Mischo, H.E., Gómez-González, B., Grzechnik, P., Rondón, A.G., Wei, W., Steinmetz, L., Aguilera, A., and Proudfoot, N.J. (2011). Yeast Sen1 helicase protects the genome from transcription-associated instability. Molecular Cell *41*, 21-32.

Mozzetta, C., Pontis, J., Fritsch, L., Robin, P., Portoso, M., Proux, C., Margueron, R., and Ait-Si-Ali, S. (2014). The histone H3 lysine 9 methyltransferases G9a and GLP regulate polycomb repressive complex 2-mediated gene silencing. Molecular Cell *53*, 277-289.

Murayama, A., Ohmori, K., Fujimura, A., Minami, H., Yasuzawa-Tanaka, K., Kuroda, T., Oie, S., Daitoku, H., Okuwaki, M., Nagata, K.*, et al.* (2008). Epigenetic control of rDNA loci in response to intracellular energy status. Cell *133*, 627-639.

Nadel, J., Athanasiadou, R., Lemetre, C., Wijetunga, N.A., Broin, P.Ó., Sato, H., Zhengdong, Z., Jeddeloh, J., Montagna, C., Golden, A.*, et al.* (2015). RNA:DNA hybrids in the human genome have distinctive nucleotide characteristics, chromatin composition, and transcriptional relationships. Epigenetics & Chromatin *8*, 1-19.

Parajuli, S., Teasley, D.C., Murali, B., Jackson, J., Vindigni, A., and Stewart, S.A. (2017). Human ribonuclease H1 resolves R-loops and thereby enables progression of the DNA replication fork. The Journal of biological chemistry *292*, 15216-15224.

Peng, J.C., and Karpen, G.H. (2007). H3K9 methylation and RNA interference regulate nucleolar organization and repeated DNA stability. Nature Cell Biology *9*, 25-35.

Purandare, N., Somayajulu, M., Hüttemann, M., Grossman, L.I., and Aras, S. (2018). The cellular stress proteins CHCHD10 and MNRR1 (CHCHD2): Partners in mitochondrial and nuclear function and dysfunction. The Journal of biological chemistry *293*, 6517-6529.

Rahman, S., and Islam, R. (2011). Mammalian Sirt1: insights on its biological functions. Cell Communication & Signaling *9*, 11-18.

Rodriguez-Corona, U., Sobol, M., Carlos Rodriguez-Zapata, L., Hozak, P., and Castano, E. (2015). Fibrillarin from Archaea to human. BIOLOGY OF THE CELL *107*, 159-174.

Rolland, T., Taşan, M., Charloteaux, B., Pevzner, Samuel J., Zhong, Q., Sahni, N., Yi, S., Lemmens, I., Fontanillo, C., Mosca, R.*, et al.* (2014). A proteome-scale map of the human interactome network. Cell *159*, 1212-1226.

Roopra, A., Qazi, R., Schoenike, B., Daley, T.J., and Morrison, J.F. (2004). Localized domains of G9a-mediated histone methylation are required for silencing of neuronal genes. Molecular Cell *14*, 727-738.

Shen, W., Sun, H., De Hoyos, C.L., Bailey, J.K., Liang, X.-H., and Crooke, S.T. (2017). Dynamic nucleoplasmic and nucleolar localization of mammalian RNase H1 in response to RNAP I transcriptional R-loops. Nucleic acids research *45*, 10672-10692.

Sherf, B.A., Navarro, S.L., Hannah, R.R., and Wood, K.V. (1996). Dual-Luciferase TM Reporter Assay: An advanced co-reporter technology integrating firefly and renilla luciferase assays. Promega Notes Magazine.

Shivji, M.K.K., Renaudin, X., Williams, Ç.H., and Venkitaraman, A.R. (2018). BRCA2 regulates

transcription elongation by RNA Polymerase II to prevent R-Loop accumulation. Cell Reports *22*, 1031-1039.

Skourti-Stathaki, K., Kamieniarz-Gdula, K., and Proudfoot, N.J. (2014). R-loops induce repressive chromatin marks over mammalian gene terminators. Nature *516*, 436-439.

Skourti-Stathaki, K., and Proudfoot, N.J. (2014). A double-edged sword: R loops as threats to genome integrity and powerful regulators of gene expression. Genes and Development *28*, 1384-1396.

Solomon, J.M., Pasupuleti, R., Xu, L., McDonagh, T., Curtis, R., DiStefano, P.S., and Huber, L.J. (2006). Inhibition of SIRT1 catalytic activity increases p53 acetylation but does not alter cell survival following DNA damage. Molecular and Cellular Biology *26*, 28-38.

Song, C., Voit, R., Grummt, I., and Hotz-Wagenblatt, A. (2017). SIRT7 and the DEAD-box helicase DDX21 cooperate to resolve genomic R loops and safeguard genome stability. Genes and Development *31*, 1370-1381.

Suzuki, Y., Holmes, J.B., Cerritelli, S.M., Sakhuja, K., Crouch, R.J., Minczuk, M., and Holt, I.J. (2010). An upstream open reading frame and the context of the two AUG codons affect the abundance of mitochondrial and nuclear RNase H1. Molecular and Cellular Biology *30*, 5123-5134.

Tachibana, M., Matsumura, Y., Fukuda, M., Shinkai, Y., and Kimura, H. (2008). G9a/GLP complexes independently mediate H3K9 and DNA methylation to silence transcription. EMBO Journal *27*, 2681-2690.

Tachibana, M., Ueda, J., Fukuda, M., Shinkai, Y., Sugimoto, K., Nozaki, M., Ohta, T., Ohki, M., Takeda, N., Niida, H.*, et al.* (2002). G9a histone methyltransferase plays a dominant role in euchromatic histone H3 lysine 9 methylation and is essential for early embryogenesis. Genes and Development *16*, 1779-1791.

Tachibana, M., Ueda, J., Fukuda, M., Shinkai, Y., Takeda, N., Ohta, T., Iwanari, H., Sakihama, T., Kodama, T., and Hamakubo, T. (2005). Histone methyltransferases G9a and GLP form heteromeric complexes and are both crucial for methylation of euchromatin at H3-K9. Genes and Development *19*, 815-826.

Tuduri, S., Crabbé, L., Conti, C., Tourrière, H., Holtgreve-Grez, H., Jauch, A., Pantesco, V., De Vos, J., Thomas, A., Theillet, C.*, et al.* (2009). Topoisomerase I suppresses genomic instability by preventing interference between replication and transcription. Nature Cell Biology *11*, 1315-1324.

Uruci, S., Lo, C.S.Y., Wheeler, D., and Taneja, N. (2021). R-Loops and Its Chro-Mates: The Strange Case of Dr. Jekyll and Mr. Hyde. International journal of molecular sciences *22*.

Vaquero, A., Scher, M., Lee, D., Erdjument-Bromage, H., Tempst, P., and Reinberg, D. (2004). Human SirT1 interacts with histone H1 and promotes formation of facultative heterochromatin. Molecular Cell *16*, 93-105.

Voit, R., Seiler, J., and Grummt, I. (2015). Cooperative action of Cdk1/cyclin B and SIRT1 is required for mitotic repression of rRNA synthesis. PLoS Genetics *11*, 1-17.

Wahba, L., Amon, Jeremy D., Koshland, D., and Vuica-Ross, M. (2011). RNase H and multiple RNA biogenesis factors cooperate to prevent RNA:DNA hybrids from generating genome instability. Molecular Cell *44*, 978-988.

Wang, L., Xu, S., Lee, J.-E., Baldridge, A., Grullon, S., Ge, K., and Peng, W. (2013). Histone H3K9 methyltransferase G9a represses PPARγ expression and adipogenesis. EMBO Journal *32*, 45-59.

Wu, H., Lima, W.F., and Crooke, S.T. (1998). Molecular cloning and expression of cDNA for human RNase H. Antisense and Nucleic Acid Drug Development *8*, 53-61.

Xu, W., Xu, H., Li, K., Fan, Y., Liu, Y., Yang, X., and Sun, Q. (2017). The R-loop is a common chromatin

feature of the *Arabidopsis* genome. Nature Plants *3*, 704-714.
Yang, Y., McBride, Kevin M., Hensley, S., Lu, Y., Chedin, F., and Bedford, Mark T. (2014). Arginine methylation facilitates the recruitment of TOP3B to chromatin to prevent R Loop accumulation. Molecular Cell *53*, 484-497.
You, Z., Jiang, W.-X., Qin, L.-Y., Gong, Z., Wan, W., Li, J., Wang, Y., Zhang, H., Peng, C., Zhou, T.*, et al.* (2019). Requirement for p62 acetylation in the aggregation of ubiquitylated proteins under nutrient stress. Nature Communications *10*, 1-14.
Yuan, J., Chang, S.-Y., Yin, S.-G., Liu, Z.-Y., Cheng, X., Liu, X.-J., Jiang, Q., Gao, G., Lin, D.-Y., Kang, X.-L.*, et al.* (2020). Two conserved epigenetic regulators prevent healthy ageing. Nature *579*, 118-122.
Yuan, X., Feng, W., Imhof, A., Grummt, I., and Zhou, Y. (2007). Activation of RNA Polymerase I transcription by Cockayne Syndrome Group B protein and Histone Methyltransferase G9a. Molecular Cell *27*, 585-595.
Yuan, Y., Wang, Q., Paulk, J., Kubicek, S., Kemp, M.M., Adams, D.J., Shamji, A.F., Wagner, B.K., and Schreiber, S.L. (2012). A small-molecule probe of the histone methyltransferase G9a induces cellular senescence in pancreatic adenocarcinoma. ACS chemical biology *7*, 1152-1157.
Zeller, P., Padeken, J., van Schendel, R., Kalck, V., Tijsterman, M., and Gasser, S.M. (2016). Histone H3K9 methylation is dispensable for *Caenorhabditis elegans* development but suppresses RNA:DNA hybrid-associated repeat instability. Nature genetics *48*, 1385-1395.
Zentner, G.E., Saiakhova, A., Manaenkov, P., Adams, M.D., and Scacheri, P.C. (2011). Integrative genomic analysis of human ribosomal DNA. Nucleic acids research *39*, 4949-4960.
Zhang, X., Chiang, H.-C., Wang, Y., Zhang, C., Smith, S., Zhao, X., Nair, S.J., Michalek, J., Jatoi, I., Lautner, M.*, et al.* (2017). Attenuation of RNA polymerase II pausing mitigates BRCA1-associated R-loop accumulation and tumorigenesis. Nature Communications *8*, 1-12.
Zheng, Y., Liu, A., Wang, Z.-J., Cao, Q., Wang, W., Lin, L., Ma, K., Zhang, F., Wei, J., Matas, E.*, et al.* (2019). Inhibition of EHMT1/2 rescues synaptic and cognitive functions for Alzheimer's disease. Brain: A Journal of Neurology *142*, 787-807.
Zhou, H., Li, L., Wang, Q., Hu, Y., Zhao, W., Gautam, M., and Li, L. (2020). H3K9 demethylation-induced R-Loop accumulation is linked to disorganized nucleoli. Frontiers in Genetics *11*.
Zhou, H., Wang, Y., Wang, Q., Li, L., Hu, Y., Wu, Y., Gautam, M., and Li, L. (2021). R-loops mediate transcription-associated formation of human rDNA secondary constrictions. Journal of cellular biochemistry.

Figure legends

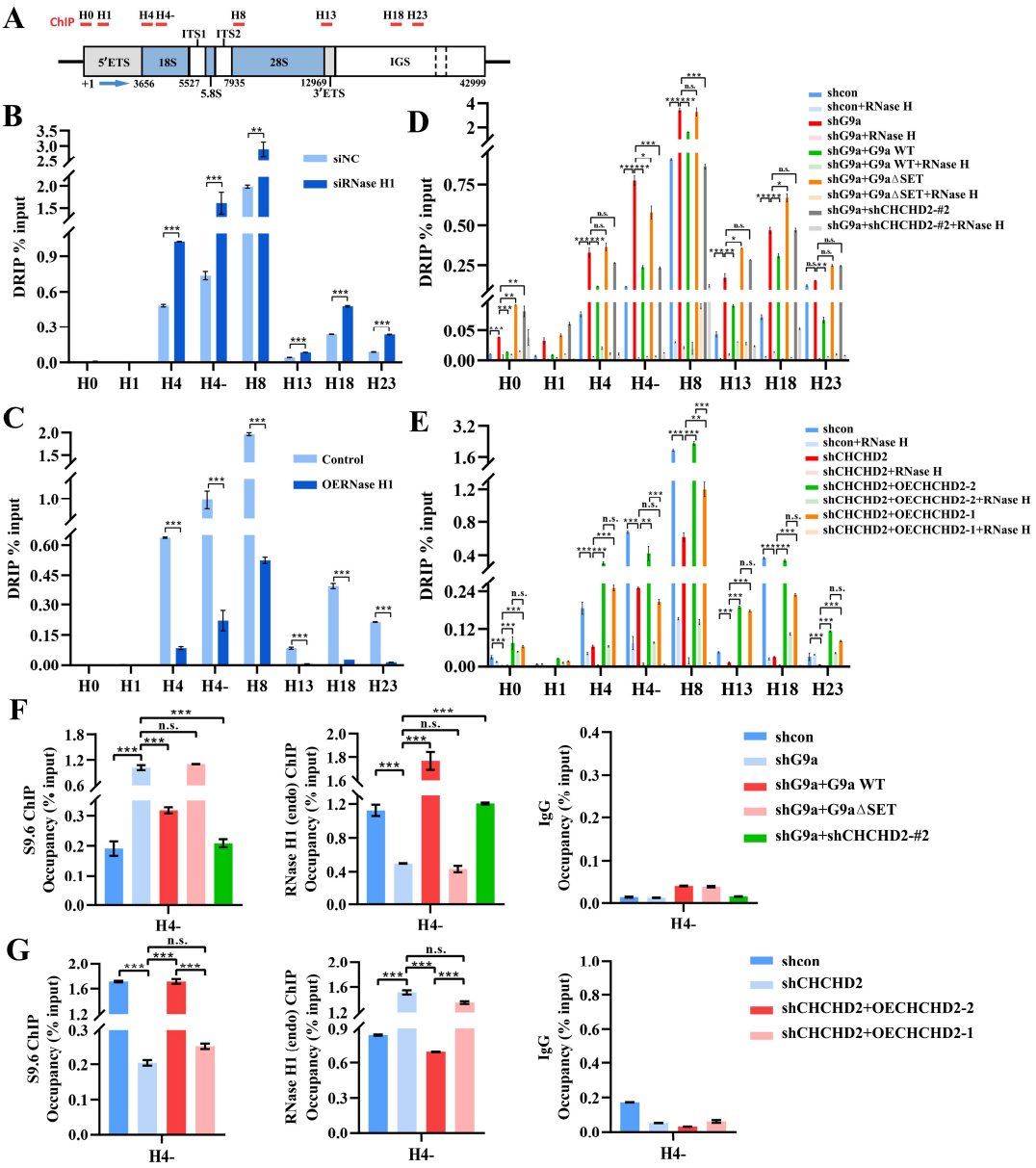

Figure 1 The effect of G9a & CHCHD2 on the R-loop formation and the recruitment of RNase H1 at the rDNA locus.

(A) The structure of the human rDNA repeat. The locations of ChIP primer pairs (H0, H0.02, H4-, H8, H13, H23, H32, UCE, CORE and H42.9) are shown above the diagram of the human rDNA repeat. **(B)** DRIP analysis at the rDNA region in HeLa cells after transfection with RNase H1 short-interfering RNA (siRNase H1) for 48 h. The HeLa cells were used as the control group after transfection with negative control RNA oligo (NC). **(C)** DRIP analysis at the rDNA region in HeLa cells after transfection with pcDNA3.1-3flag-RNase H1 (OERNase H1) for 48 h. The HeLa cells were used as the control group after transfection with the pcDNA3.1-3flag empty vector. **(D)** DRIP analysis at the rDNA region in stable shG9a HeLa cells with or without in vitro RNase H treatment after transfection with pEGFP-G9a (G9a WT), pEGFP-G9a-ΔSET (G9a ΔSET) or pLKO.1-shCHCHD2-#2 (shCHCHD2-#2) for 48 h. The pEGFP-N1 and the pLKO.1 empty vector was used as the negative control and was added respectively to maintain equal amounts of total transfected DNA. **(E)** DRIP analysis at the rDNA region in

stable shCHCHD2 HeLa cells with or without in vitro RNase H treatment after transfection with pcDNA3.1-3flag-CHCHD2-isoform1(OECHCHD2-1) or pcDNA3.1-3flag-CHCHD2-isoform2 (OECHCHD2-2) for 48 h. The pcDNA3.1-3flag empty vector was used as the negative control and was added to maintain equal amounts of total transfected DNA. The y-axis indicated the ratio of the relative quantities of R-loop in each group. Relative values were normalized to the input. The x-axis indicated different regions of rDNA amplicons. All results represent at least three independent experiments (±SD). * $P < 0.05$, ** $P < 0.01$, *** $P < 0.001$, n. s. means not significant, measured by the *t*-test. **(F)** S9.6 ChIP and endogenous RNase H1 ChIP were used to detect the R-loop and RNase H1 occupancy at rDNA in HeLa cells after the same treatment as shown in figure 1D. **(G)** S9.6 ChIP and endogenous RNase H1 ChIP were used to detect the R-loop and RNase H1 occupancy at rDNA in HeLa cells after the same treatment as shown in figure 1E. Relative values were normalized to the input. The x-axis indicated the region H4- of rDNA amplicons. The result represents at least three independent experiments (±SD). * $P < 0.05$, ** $P < 0.01$, *** $P < 0.001$, n. s. means not significant, measured by the *t*-test.

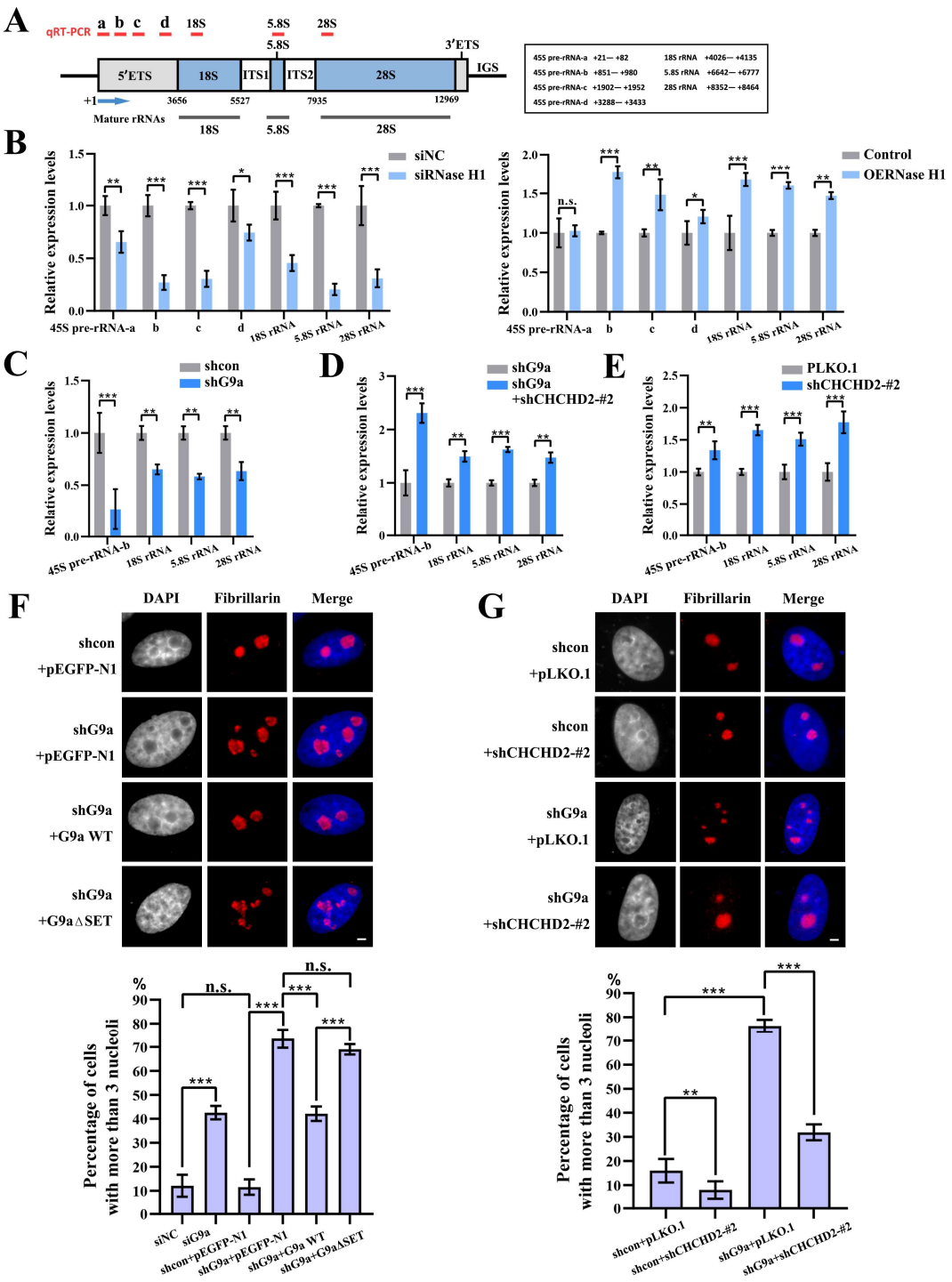

Figure 2 The effect of G9a & CHCHD2 on rRNA transcription and fragmented nucleoli. **(A)** Diagram of the human rRNA coding locus and location of real-time quantitative PCR(RT-qPCR)primers. **(B)** RT-qPCR was used to detect the incomplete 5'ETS transcripts (45S-pre-rRNA-a, b, c and d) and the mature rRNA expressions (18S, 5.8S and 28S) in HeLa cells after transfection with RNase H1 short-interfering RNA (siRNase H1) and pcDNA3.1-3flag-RNase H1 (OERNase H1) for 48 h. The HeLa cells were used as the control group after transfection with negative control RNA oligo (NC) and the pcDNA3.1-3flag empty vector. **(C)** RT-qPCR was used to detect the incomplete 5'ETS transcripts (45S-pre-rRNA-b) and the mature rRNA expressions (18S, 5.8S and 28S) in stable shG9a HeLa cells and shcon HeLa cells. **(D)** RT-qPCR was used to detect the incomplete 5'ETS transcripts and the mature rRNA expressions in stable shG9a HeLa cells after transfection with shCHCHD2-#2 for 48 h. The

pLKO.1 empty vector was used as the negative control and was added to maintain equal amounts of total transfected DNA. **(E)** RT-qPCR was used to detect the incomplete 5'ETS transcripts and the mature rRNA expressions in HeLa cells after transfection with shCHCHD2-#2 for 48 h. The pLKO.1 empty vector was used as the negative control and was added to maintain equal amounts of total transfected DNA. Expression values were normalized to the gene *GAPDH*. The relative expression ratio of each sample was compared with untreated cells, expression value of which was assigned as 1. The error bars represent $2^{-\Delta\Delta CT} \pm$ the SD of three independent experiments and each experiment was repeated three times. The above results are expressed as * $P < 0.05$, ** $P < 0.01$, *** $P < 0.001$, and n. s. means no significance, measured by the *t*-test. **(F)** Upper panel: Stable shG9a HeLa cells after transfection with pEGFP-G9a (G9a WT) or pEGFP-G9a-ΔSET (G9a ΔSET) for 48 h and then indirect immunofluorescence staining with the anti-fibrillarin antibody was used to detect the nucleoli. The pEGFP-N1 empty vector was used as the negative control and was added to maintain equal amounts of total transfected DNA in shcon HeLa cells and stable shG9a HeLa cells. Bar = 3 μm. Lower panel: Percentages of interphase nuclei with more than three fragmented nucleoli after transfection with G9a WT or G9a ΔSET for 48 h. **(G)** Upper panel: The shcon HeLa cells and stable shG9a HeLa cells after transfection with pLKO.1-shCHCHD2-#2 (shCHCHD2-#2) for 48 h and then indirect immunofluorescence staining with the anti-fibrillarin antibody was used to detect the nucleoli. The pLKO.1 empty vector was used as the negative control and was added to maintain equal amounts of total transfected DNA in shcon HeLa cells and stable shG9a HeLa cells. Bar = 3 μm. Lower panel: Percentages of interphase nuclei with more than three fragmented nucleoli after transfection with shCHCHD2-#2 for 48 h. The number of evaluated nuclei in each group was 500. All results are expressed as * $P < 0.05$, ** $P < 0.01$, *** $P < 0.001$, and n. s. means no significance, measured by the *t*-test.

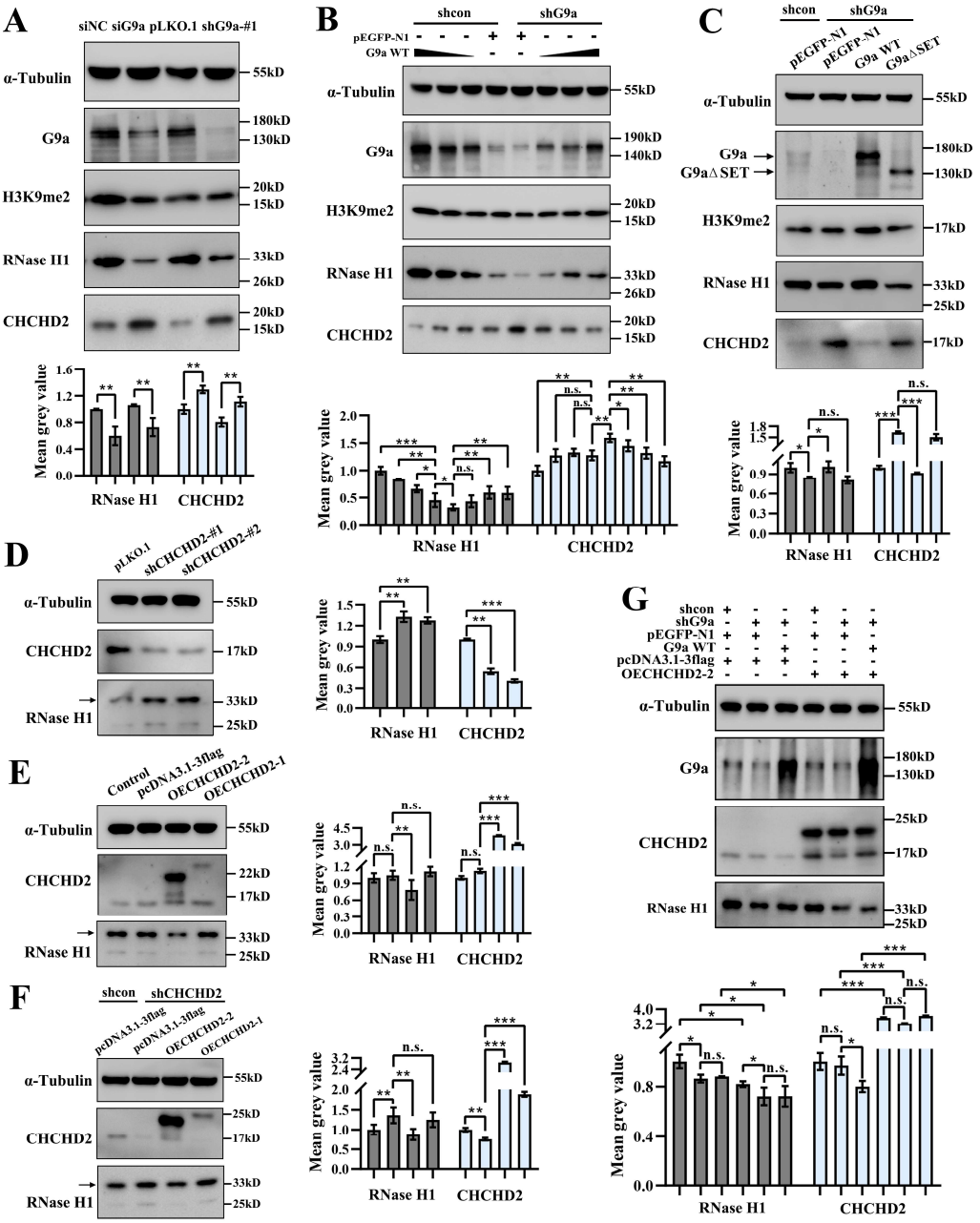

Figure 3 G9a and CHCHD2 precisely regulate the expression of RNase H1.

(A) Western blot analysis of RNase H1, CHCHD2, G9a and H3K9me2 expression in HeLa cells after transfection with G9a short-interfering RNA (siG9a) and shG9a-#1 for 48 h. The HeLa cells were used as the control group after transfection with negative control RNA oligo (NC) and the pLKO.1 empty vector. RNase H1, CHCHD2 and G9a levels were quantified to the level of α-tubulin. H3K9me2 levels were quantified to the level of H3. **(B)** Western blot analysis of RNase H1, CHCHD2, G9a and H3K9me2 expression in stable shG9a HeLa cells and shcon HeLa cells after transfection with G9a WT (0.375, 0.5 and 0.625 μg) for 48 h. The pEGFP-N1 empty vector was added to as the control group. RNase H1, CHCHD2 and G9a levels were quantified to the level of α-tubulin. H3K9me2 levels were quantified to the level of H3. **(C)** Western blot analyses showed the relative expression levels of RNase H1, CHCHD2, G9a and H3K9me2 in G9a knockdown, G9a WT and G9a SET domain deleted rescued HeLa cells. The pEGFP-N1 empty vector was used as the negative control and was added to maintain equal amounts of total transfected DNA. The expression levels of RNase H1, CHCHD2 and G9a are quantified to α-tubulin. H3K9me2

levels were quantified to the level of H3. In the above groups, the relative mean gray value of RNase H1 and CHCHD2 were shown in the lower panel. **(D)** Western blot analysis of RNase H1 and CHCHD2 expression in HeLa cells after transfection with pLKO.1-shCHCHD2-#1 (shCHCHD2-#1) and shCHCHD2-#2 for 48 h. The pLKO.1 empty vector was used as the negative control and was added to maintain equal amounts of total transfected DNA. RNase H1 and CHCHD2 levels were quantified to the level of α-tubulin. **(E)** Western blot analysis of RNase H1 and CHCHD2 expression in HeLa cells after transfection with OECHCHD2-1 and OECHCHD2-2 for 48 h. The pcDNA3.1-3flag empty vector was used as the negative control and was added to maintain equal amounts of total transfected DNA. RNase H1 and CHCHD2 levels were quantified to the level of α-tubulin. **(F)** Western blot analyses showed the relative expression levels of RNase H1 and CHCHD2 in CHCHD2 knockdown, CHCHD2-isoform1 and CHCHD2-isoform2 rescued HeLa cells. The pcDNA3.1-3flag empty vector was used as the negative control and was added to maintain equal amounts of total transfected DNA. The expression levels of RNase H1 and CHCHD2 are quantified to α-tubulin. In the above groups, the relative mean gray value of RNase H1 and CHCHD2 were shown in the right panel. **(G)** Western blot analyses showed the relative expression levels of RNase H1, CHCHD2 and G9a in shcon HeLa cells, stable shG9a HeLa cells and G9a WT rescued shG9a HeLa cells after transfection with OECHCHD2-2 for 48 h. The pEGFP-N1 and the pcDNA3.1-3flag empty vectors were used as the negative control and were added to maintain equal amounts of total transfected DNA. All the protein levels were quantified and normalized to the level of α-tubulin. The relative mean gray value of RNase H1 and CHCHD2 were shown in the lower panel. Each experiment was repeated three times, and the average value and SD are shown. Data are expressed as * $P < 0.05$, ** $P < 0.01$, *** $P < 0.001$, and n. s. means no significance, measured by the *t*-test.

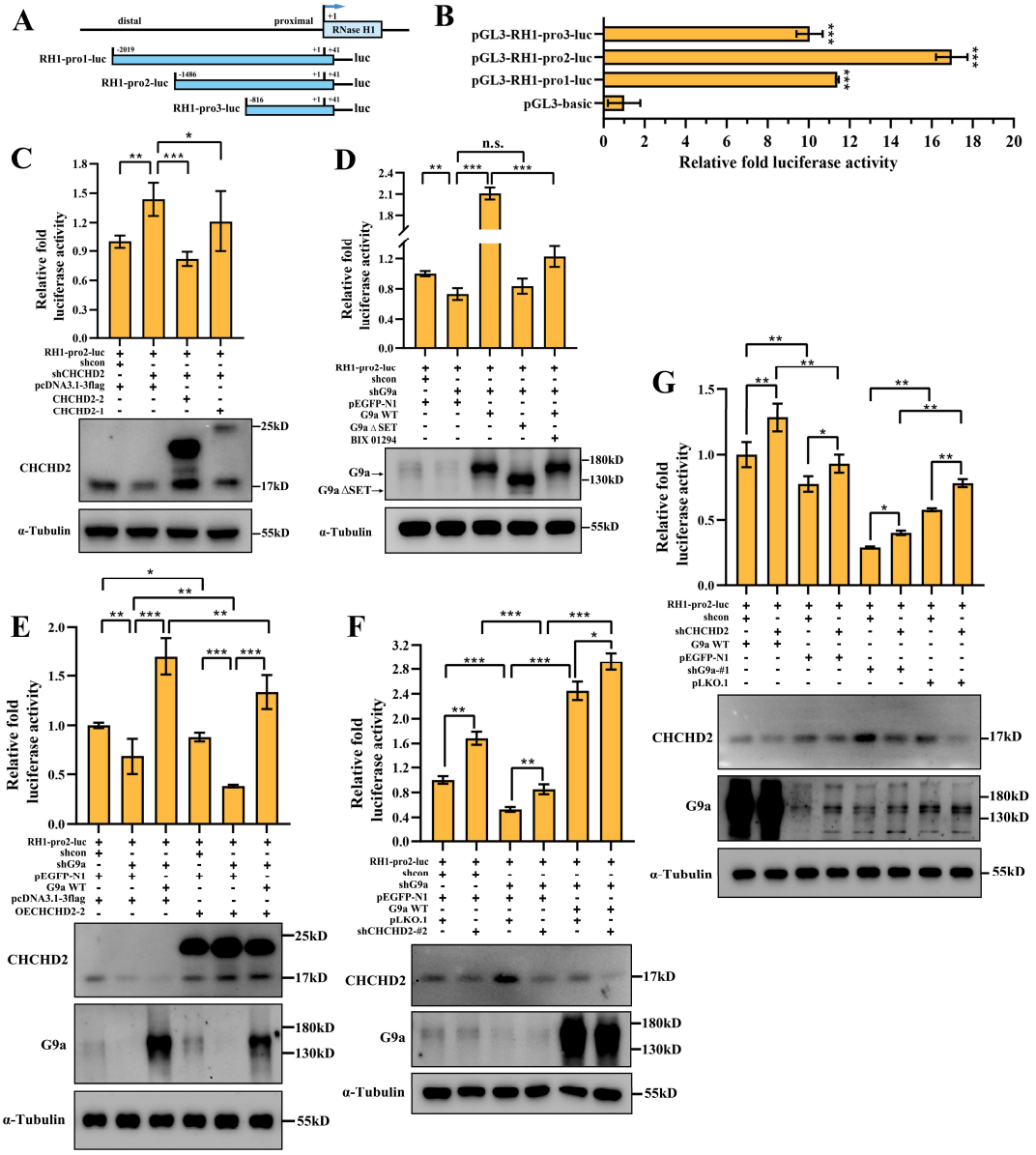

Figure 4 G9a & CHCHD2 function with each other and mediate transcriptional regulation through RNase H1 promoter

(A) Schematic representation of the different lengths of the RNase H1 promoters, constructed to form the pGL3 luciferase vector. The "+1" represents the transcription start site. **(B)** RNase H1 promoter activity analysis. **(C)** Stable shCHCHD2 HeLa cells were co-transfected with the pGL3-RNase H1 promoter, OECHCHD2-1 and OECHCHD2-2, along with the TK-Renilla luciferase expression plasmid (phRL-TK). The pcDNA3.1-3flag empty vector was used as the negative control and was added to maintain equal amounts of total transfected DNA. Cell extracts were assayed for luciferase activity. CHCHD2 overexpression or knockdown was confirmed by western blot analysis. **(D)** Stable shG9a HeLa cells were co-transfected with the pGL3- RNase H1 promoter, G9a WT and G9a ΔSET, along with the phRL-TK. Twenty-four hours after transfection, G9a WT rescued HeLa cells were treated with BIX01294 (10 μM) for 24 h. The pEGFP-N1 empty vector was used as the negative control and was added to maintain equal amounts of total transfected DNA. Cell extracts were assayed for luciferase activity. G9a overexpression or knockdown was confirmed by western blot analysis. **(E)** Shcon HeLa cells, stable shG9a HeLa cells and G9a WT rescued shG9a HeLa cells were co-transfected with the pGL3- RNase H1 promoter and OECHCHD2-2, along with

the phRL-TK. The pEGFP-N1 and the pcDNA3.1-3flag empty vector were used as control and were added to maintain equal amounts of total transfected DNA. Cell extracts were assayed for luciferase activity. **(F)** The shcon HeLa cells, stable shG9a HeLa cells and G9a WT rescued shG9a HeLa cells were co-transfected with the pGL3-RNase H1 promoter and shCHCHD2-#2, along with the phRL-TK. The pEGFP-N1 and the pLKO.1 empty vector were used as control and were added to maintain equal amounts of total transfected DNA. Cell extracts were assayed for luciferase activity. **(G)** Shcon HeLa cells and stable shCHCHD2 HeLa cells were co-transfected with the pGL3-RNase H1 promoter, G9a WT and shG9a-#1, along with the phRL-TK. The pEGFP-N1 and the pLKO.1 empty vector were used as control and were added to maintain equal amounts of total transfected DNA. Cell extracts were assayed for luciferase activity. Firefly luciferase activity levels were normalized to those of the Renilla luciferases. Expression of the transfected constructs is shown in the immunoblot analysis. Each *P*-value represents the mean of three replicates from a single assay. All data are representative of at least three independent experiments and are presented as means ±SD. All the results are expressed as * $P < 0.05$, ** $P < 0.01$, *** $P < 0.001$, and n. s. means no significance, measured by the *t*-test.

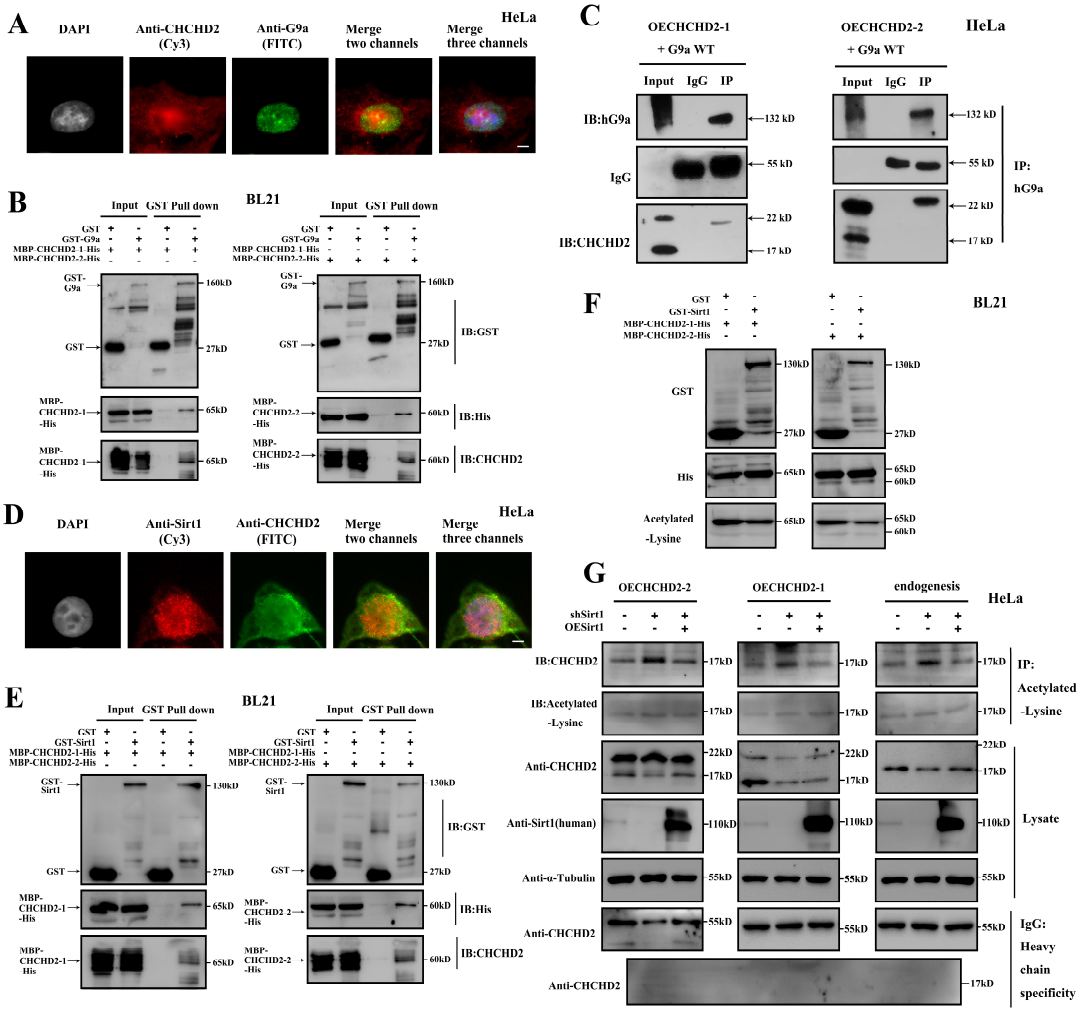

Figure 5 CHCHD2 can interact with both G9a and Sirt1.

(A) CHCHD2 and G9a were detected by indirect immunofluorescence staining with an antibody against CHCHD2 (CHCHD2, Cy3) and an antibody against G9a (G9a, FITC) in interphase nuclei of Hela cells. **(B)** GST pull-down assay showing the interaction of purified MBP-CHCHD2-His and GST-G9a from BL21. GST-G9a pull-down products were analyzed by western blot with anti-His and anti-CHCHD2 antibodies. **(C)** HeLa cells were co-transfected with G9A WT, OECHCHD2-1 and OECHCHD2-2 constructs. Anti-G9a immunoprecipitates were analyzed by western blot with anti-CHCHD2 antibody. **(D)** CHCHD2 and Sirt1 were detected by indirect immunofluorescence staining with an antibody against CHCHD2 (CHCHD2, FITC) and an antibody against Sirt1 (Sirt1, Cy3) in interphase nuclei of Hela cells. **(E)** GST pull-down assay showing the interaction of purified MBP-CHCHD2-His and GST-Sirt1 from BL21. GST-Sirt1 pull-down products were analyzed by western blot with anti-His and anti-CHCHD2 antibodies. **(F)** In vitro CHCHD2 acetylation assay. Purified MBP-CHCHD2-His was incubated with GST-Sirt1 from BL21, in the absence of acetyl-CoA. CHCHD2 acetylation was analyzed by western blot using anti-Acetylated-Lysine. **(G)** Acetylation of CHCHD2-isoform1, CHCHD2-isoform2 and endogenous CHCHD2 in stable shSirt1 cells after transfection with OESirt1 for 48h. The pcDNA3.1-3flag empty vector was used as the negative control and was added to maintain equal amounts of total transfected DNA. CHCHD2 acetylation was analyzed by immunoprecipitation with anti-Acetylated-Lysine antibody followed by western blot for CHCHD2. Expression of CHCHD2, Sirt1 and α-tubulin were shown in the lysate immunoblot analysis.

Immunoblotting results of IgG control group incubated with anti-CHCHD2 antibody shown by heavy chain specific secondary antibody.

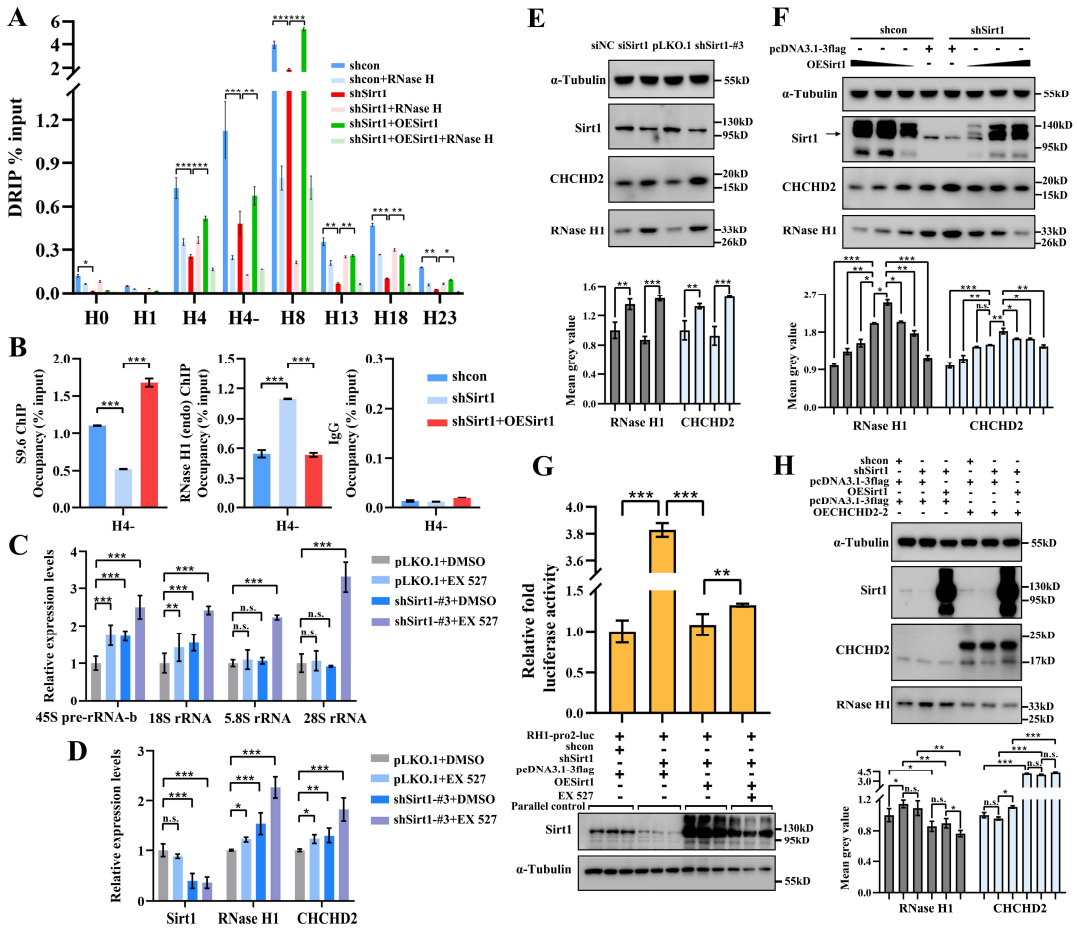

Figure 6 Sirt1 functions as a co-repressor in regulating RNase H1.

(A) DRIP analysis at the rDNA region in stable shSirt1 HeLa cells with or without in vitro RNase H treatment after transfection with pcDNA3.1-3flag-Sirt1 (OESirt1) for 48 h. The pcDNA3.1-3flag empty vector was used as the negative control and was added to maintain equal amounts of total transfected DNA. The y-axis indicated the ratio of the relative quantities of R-loop in each group. Relative values were normalized to the input. The x-axis indicated different regions of rDNA amplicons. The result represents at least three independent experiments (±SD). * $P < 0.05$, ** $P < 0.01$, *** $P < 0.001$, n. s. means not significant, measured by the *t*-test. **(B)** S9.6 ChIP and endogenous RNase H1 ChIP were used to detect the R-loop and RNase H1 occupancy at rDNA in HeLa cells after the same treatment as shown in figure 6A. Relative values were normalized to the input. The x-axis indicated the region H4- of rDNA amplicons. The result represents at least three independent experiments (±SD). * $P < 0.05$, ** $P < 0.01$, *** $P < 0.001$, n. s. means not significant, measured by the *t*-test. **(C)** RT-qPCR was used to detect the incomplete 5'ETS transcripts (45S-pre-rRNA-b) and the mature rRNA expressions (18S, 5.8S and 28S) in HeLa cells after treatment with 10 μM EX 527 or transfection with pLKO.1-shSirt1-#3 (shSirt1-#3) for 48 h. The pLKO.1 empty vector was used as the negative control and was added to maintain equal amounts of total transfected DNA. The same proportion of DMSO as the 10 μM EX 527 group were added to the rest of the non-inhibitor treatment group which were used as the solvent control. **(D)** RT-qPCR was used to detect the RNase H1, CHCHD2 and Sirt1 expression in HeLa cells after the same treatment as shown in figure 6C. Expression values were normalized to the gene *GAPDH*. The relative expression ratio of each sample was compared with untreated cells, expression value of which was assigned as 1. The error bars represent $2^{-\Delta\Delta CT} \pm$ the SD of three independent experiments and each experiment was repeated three times. The above results are expressed as * $P < 0.05$, ** $P < 0.01$, *** $P < 0.001$, and n. s. means no significance, measured by the *t*-test. **(E)** Western blot analysis of RNase

H1, CHCHD2 and Sirt1 expression in HeLa cells after transfection with Sirt1 short-interfering RNA (siSirt1) and pLKO.1-shSirt1-#3 (shSirt1-#3) for 48 h. The HeLa cells were used as the control group after transfection with negative control RNA oligo (NC) and the pLKO.1 empty vector. RNase H1, CHCHD2 and Sirt1 levels were quantified to the level of α-tubulin. **(F)** Western blot analysis of RNase H1, CHCHD2 and Sirt1 expression in stable shSirt1 HeLa cells and shcon HeLa cells after transfection with OESirt1 (0.375, 0.5 and 0.625 μg) for 48 h. The pcDNA3.1-3flag empty vector was added to as the control group. RNase H1, CHCHD2 and Sirt1 levels were quantified to the level of α-tubulin. In the above groups, the relative mean gray value of RNase H1 and CHCHD2 were shown in the lower panel. Each experiment was repeated three times, and the average value and SD are shown. Data are expressed as * $P < 0.05$, ** $P < 0.01$, *** $P < 0.001$, and n. s. means no significance, measured by the *t*-test. **(G)** Stable shSirt1 HeLa cells were co-transfected with the pGL3- RNase H1 promoter, OESirt1, along with the phRL-TK. Twenty-four hours after transfection, Sirt1 rescued HeLa cells were treated with EX 527(10 μM) for 24 h. The pcDNA3.1-3flag empty vector was used as the negative control and was added to maintain equal amounts of total transfected DNA. The same proportion of DMSO as the 10 μM EX 527 group were added to the rest of the non-inhibitor treatment group which were used as the solvent control. Cell extracts were assayed for luciferase activity. Firefly luciferase activity levels were normalized to those of the Renilla luciferases. Sirt1 overexpression or knockdown was confirmed by western blot analysis. Each *P*-value represents the mean of three replicates from a single assay. All data are representative of at least three independent experiments and are presented as means ±SD. *t*-test is performed, * $P < 0.05$, ** $P < 0.01$ and *** $P < 0.001$, n. s. means not significant. **(H)** Western blot analyses showed the relative expression levels of RNase H1, CHCHD2 and Sirt1 in shcon HeLa cells, stable shSirt1 HeLa cells and Sirt1 rescued shSirt1 HeLa cells after transfection with OECHCHD2-2 for 48 h. The pcDNA3.1-3flag empty vector was used as the negative control and was added to maintain equal amounts of total transfected DNA. All the protein levels were quantified and normalized to the level of α-tubulin. The relative mean gray value of RNase H1 and CHCHD2 were shown in the lower panel. The experiment was repeated three times, and the average value and SD are shown. Data are expressed as * $P < 0.05$, ** $P < 0.01$, *** $P < 0.001$, and n. s. means no significance, measured by the *t*-test.

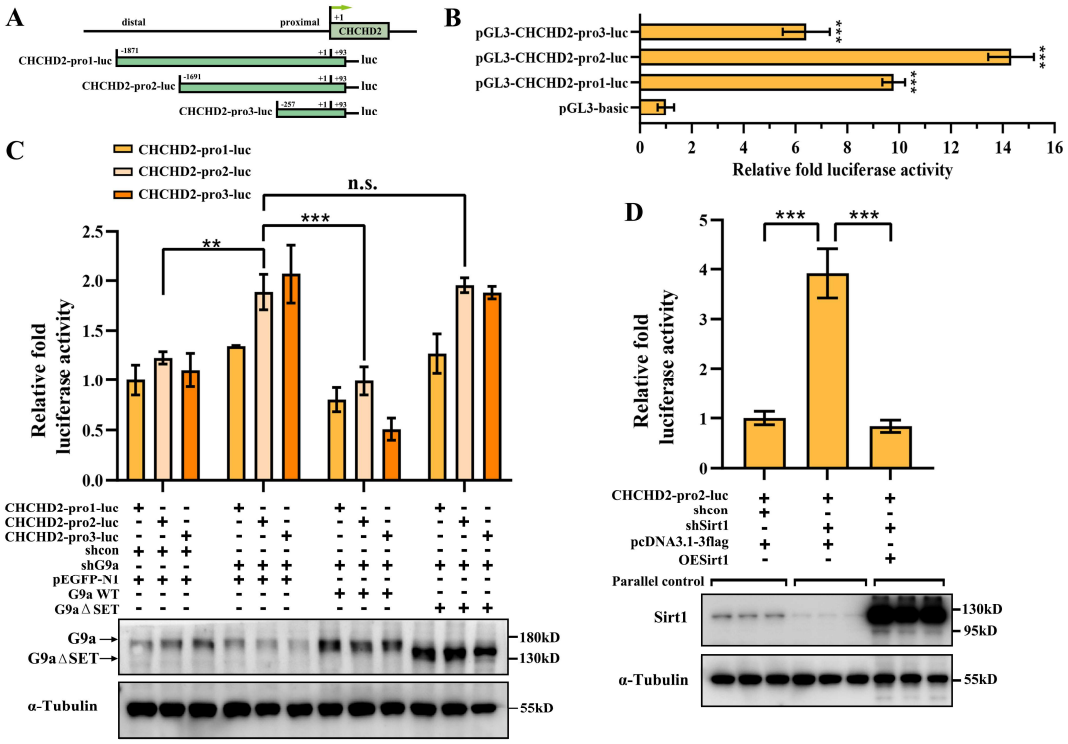

Figure 7 CHCHD2 transcriptional regulation mediated by G9a and Sirt1.

(A) Schematic representation of the different lengths of the CHCHD2 promoters, constructed to form the pGL3 luciferase vector. The "+1" represents the transcription start site. **(B)** CHCHD2 promoter activity analysis in luciferase reporter assays. **(C)** Stable shG9a HeLa cells were co-transfected with the pGL3-CHCHD2-pro1-luc, pGL3- CHCHD2-pro2-luc, pGL3- CHCHD2-pro3-luc, G9a WT and G9a ΔSET, along with the phRL-TK. The pEGFP-N1 empty vector was used as the negative control and was added to maintain equal amounts of total transfected DNA. Cell extracts were assayed for luciferase activity. G9a overexpression or knockdown was confirmed by western blot analysis in the lower panel. **(D)** Stable shSirt1 HeLa cells were co-transfected with the pGL3-CHCHD2-pro2-luc, pcDNA3.1-3flag- Sirt1 (OESirt1), along with the phRL-TK. The pcDNA3.1-3flag empty vector was used as the negative control and was added to maintain equal amounts of total transfected DNA. Cell extracts were assayed for luciferase activity. Firefly luciferase activity levels were normalized to those of the Renilla luciferases. Sirt1 overexpression or knockdown was confirmed by western blot analysis. Each *P*-value represents the mean of three replicates from a single assay. All data are representative of at least three independent experiments and are presented as means ±SD. All the results are expressed as * $P < 0.05$, ** $P < 0.01$, *** $P < 0.001$, and n. s. means no significance, measured by the *t*-test.

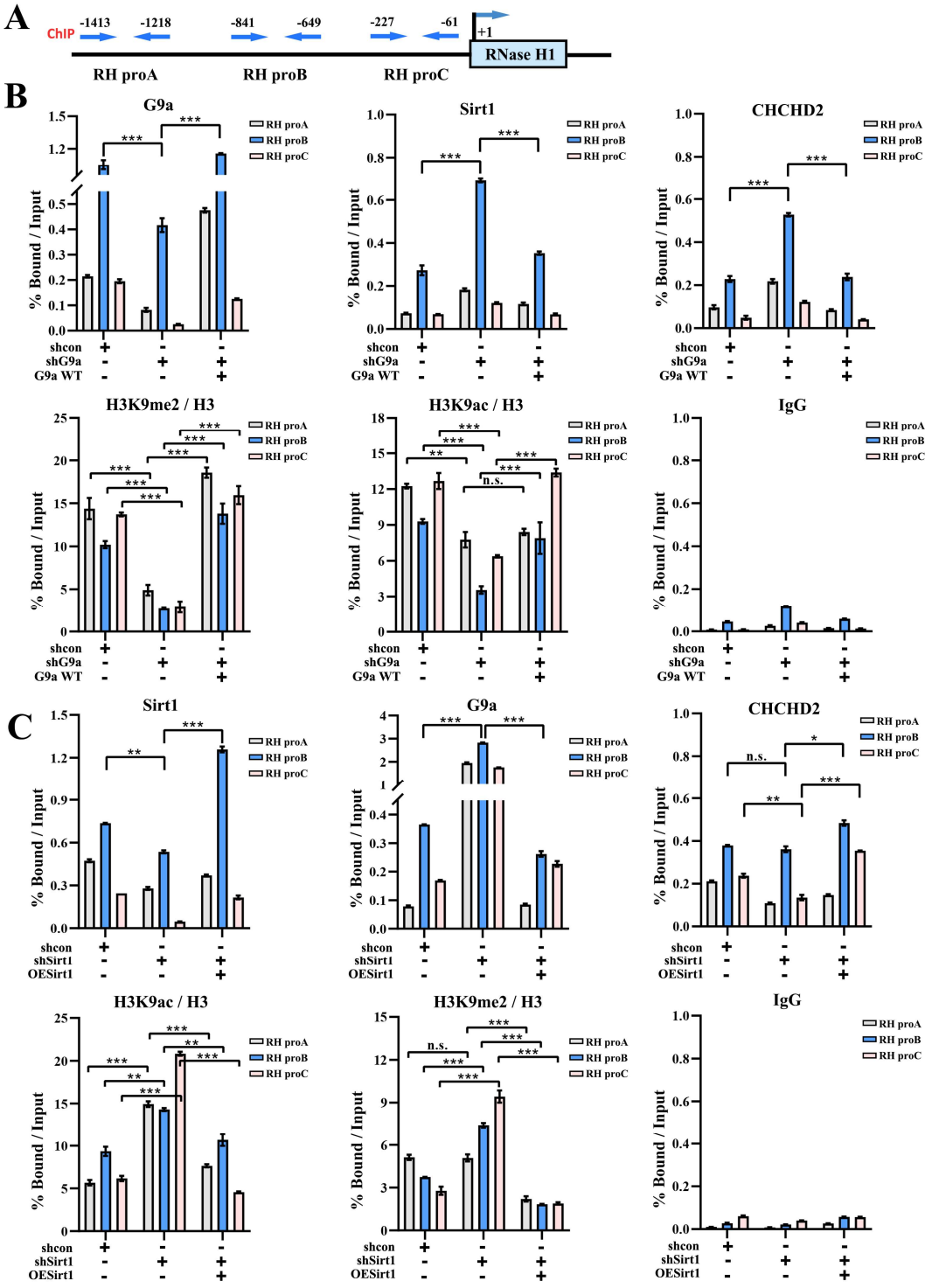

Figure 8 G9a prevents Sirt1 and CHCHD2 from being recruited to the RNase H1 promoter.

(A) Schematic diagram of primer pairs in ChIP analysis. Arrows indicate the primers used for real-time PCR amplification. **(B)** Stable shG9a HeLa cells were transfected with G9a WT. The shcon HeLa cells and stable shG9a HeLa cells which transfect with pEGFP-N1 were used as the control group. ChIP analysis was performed using anti-Sirt1, anti-G9a, anti-CHCHD2, anti-H3, anti-H3K9ac and anti-H3K9me2 antibodies, and the results were confirmed by real-time PCR. Recruitment of Sirt1, G9a and CHCHD2 to the RNase H1 promoter was normalized by input.

Relative values of H3K9ac and H3K9me2 were normalized to those of the total H3. **(C)** Stable shSirt1 HeLa cells were transfected with OESirt1. The shcon HeLa cells and stable shSirt1 HeLa cells which transfect with pcDNA3.1-3flag were used as the control group. ChIP analysis was performed using anti-Sirt1, anti-G9a, anti-CHCHD2, anti-H3, anti-H3K9ac and anti-H3K9me2 antibodies, and the results were confirmed by real-time PCR. Recruitment of Sirt1, G9a and CHCHD2 to the RNase H1 promoter was normalized by input. Relative values of H3K9ac and H3K9me2 were normalized to those of the total H3. All results represent at least three independent experiments (±SD). * $P < 0.05$, ** $P < 0.01$, *** $P < 0.001$, n. s. means not significant, measured by the *t*-test.

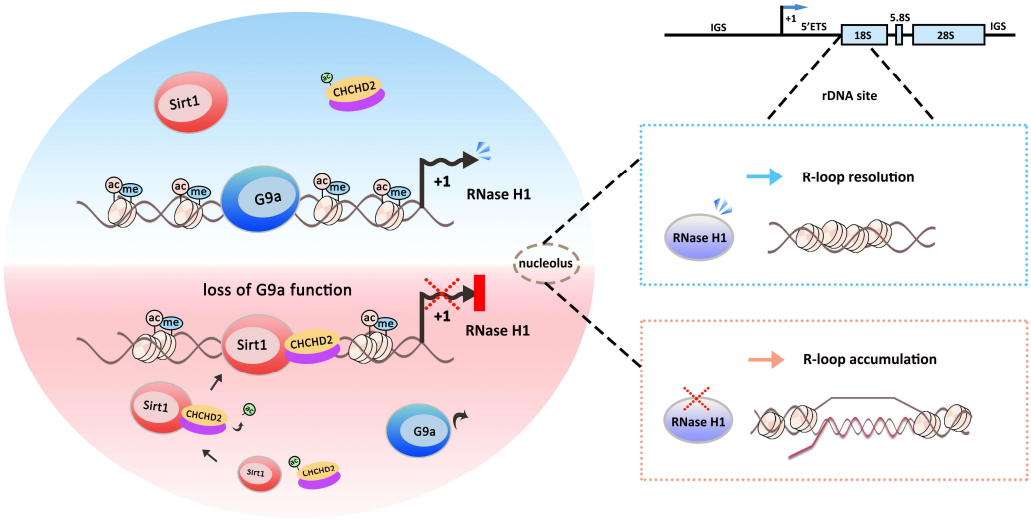

Figure 9 A model representing mechanistic link between the regulation of RNase H1 by G9a/CHCHD2/Sirt1 module and R-loop formation.

The transient R-loops formed in the active rRNA transcriptional process are degraded by RNase H1. The loss of RNase H1 function leads to the R-loop accumulation and rRNA transcriptional repression, further resulting in structurally disorganized nucleolus. G9a prevents CHCHD2 from accessing the RNase H1 promoter to induce its expression, which inhibits R-loop formation. CHCHD2 acts as a repressive transcription factor to promote R-loop enrichment at the rDNA locus by negatively regulating RNase H1. In addition, Sirt1 functions in down-regulating RNase H1 expression and increasing R-loop accumulation. CHCHD2 interacts with both G9a and Sirt1. When the function of G9a is lost, more CHCHD2 and Sirt1 are recruited to the RNase H1 promoter, and CHCHD2 tends to co-inhibit the RNase H1 expression with Sirt1. CHCHD2, G9a and Sirt1 function with each other and precisely regulate the expression of RNase H1 to maintain the steady-state balance of R-loops.

Supplementary Files

This is a list of supplementary files associated with this preprint. Click to download.

- Supplementaryinformation.docx